Submarine Groundwater Discharge-Derived Nutrient Fluxes in Eckernförde Bay (Western Baltic Sea)

M. Kreuzburg[1,2] · J. Scholten[1] · Feng-Hsin Hsu[3] · V. Liebetrau[4] · J. Sültenfuß[5] · J. Rapaglia[1] · M. Schlüter[6]

Abstract

Excess nutrient supply by the rivers and the atmosphere are considered as the major causes for the persistently poor ecological status of the Baltic Sea. More than 97% of the Baltic Sea still suffers from eutrophication due to past and present inputs of nitrogen and phosphorus. One of the poorly quantified nutrient sources in the Baltic Sea is submarine groundwater discharge (SGD). Through seepage meter deployments and a radium mass balance model, a widespread occurrence of SGD along the coastline of Eckernförde Bay was detected. Mean SGD was 21.6 cm d^{-1} with a calculated freshwater fraction of 17%. Where SGD was detected, pore water sampled by a piezometer revealed a wide range of dissolved inorganic nitrogen (DIN: 0.05–1.722 µmol L^{-1}) and phosphate (PO$_4^{3-}$: 0.03–70.5 µmol L^{-1}) concentrations. Mean DIN and PO$_4^{3-}$ concentrations in non-saline (salinity < 1) pore waters were 59 ± 68 µmol L^{-1} and 1.2 ± 1.9 µmol L^{-1}, respectively; whereas pore water with salinities > 1 revealed higher values, 113 ± 207 µmol L^{-1} and 6 ± 12 µmol L^{-1} for DIN and PO$_4^{3-}$, respectively. The nutrient concentrations along the salinity gradient do not suggest that land-derived groundwater is the definitive source of nutrients in the Baltic Sea. Still, SGD may contribute to a major autochthonous nutrient source, resulting from remineralization or dissolution processes of organic matter in the sediments. The DIN and PO$_4^{3-}$ fluxes derived from SGD rates through seepage meters are 7.9 ± 9.2 mmol m^{-2} d^{-1} and 0.5 ± 0.4 mmol m^{-2} d^{-1}, lower by a factor of ~ 2 and ~ 5 when compared to the fluxes derived with the radium mass balance model (mean DIN: 19 ± 28 mmol m^{-2} d^{-1}; mean PO$_4^{3-}$: 1.5 ± 2.7 mmol m^{-2} d^{-1}). Assuming that these mean radium-based nutrient fluxes are representative for the coastline of Eckernförde Bay, we arrive at SGD-borne nutrient fluxes of about 1 t km^{-1} y^{-1} of nitrogen and 0.2 t km^{-1} y^{-1} of phosphorous. These fluxes are lower for DIN and in the same range for phosphorus as compared to the riverine nutrient supply (DIN: 6.3 t km^{-1} y^{-1}, P: 0.2 km^{-1} y^{-1}) to the German Baltic Sea identifying SGD-borne nutrients as a secondary nutrient source to the Baltic Sea.

Introduction

Submarine groundwater discharge (SGD) is the subsurface flow of water to the coastal ocean and impacts coastal nutrient budgets world-wide (Moore 2010; Rodellas et al.

Communicated by Paul A. Montagna

V. Liebetrau was deceased during the preparation of this study.

✉ M. Kreuzburg
Matthias.Kreuzburg@uantwerpen.be

1   Institute of Geoscience, Kiel University, Kiel, Germany

2   Department of Biology, University of Antwerp, Antwerp, Belgium

3   Institute of Oceanography, National Taiwan University, Taipei, Taiwan

4   GEOMAR - Helmholtz-Zentrum Für Ozeanforschung Kiel, Kiel, Germany

5   Institute of Environmental Physics/Section of Oceanography, University of Bremen, Bremen, Germany

6   Marine Geology, Alfred Wegener Institute, Marine Geochemistry, GeosciencesBremerhaven, Germany

2015; Rocha et al. 2015; Peng et al. 2022). A recent review found that over 60% out of 200 studies reported SGD-borne nutrient fluxes exceeding nutrient riverine inputs with detrimental effects on coastal ecosystems (Santos et al. 2021). Increasing SGD-derived nitrogen availability can contribute to eutrophication, resulting in adverse impacts (Santos et al. 2009; Kotwicki et al. 2014; Seitzinger et al. 2005). SGD may drive coastal bio-productivity towards phosphorus limitation because SGD nitrogen-to-phosphorus (N/P) ratios are typically above the Redfield ratio of 16:1 (Slomp and Van Cappellen 2004; Rocha et al. 2015; Santos et al. 2021). SGD is associated with the outbreaks of harmful algal blooms (Hu et al. 2006; LaRoche et al. 1997; Lee et al. 2010) as well as coastal pollution through pesticides and heavy metals such as monomethyl mercury (Duque et al. 2020; Rahman et al. 2013; Black et al. 2009; Vaupotic et al. 2008).

Despite the poor environmental conditions with respect to the eutrophication status of marine waters of the Baltic Sea, the effects of SGD have been largely ignored. The Baltic Environment Protection Commission (HELCOM) only monitors the main nutrient transport routes (rivers and the atmosphere) and these sources are believed to have caused a tenfold extension of hypoxic areas during the past 115 years (Carstensen et al. 2014). Some modeling studies indicated that a substantial amount of water and dissolved nutrients flow unmonitored into the Baltic Sea and contribute to its eutrophication status. (Hannerz and Destouni 2006; Destouni et al. 2008). Studies in the Bay of Puck (Poland) proposed that SGD can be a major phosphorous source for the Baltic Sea (Szymczycha et al. 2012). Further studies reported SGD occurring along the coastline of the Baltic Sea, for example, input from Laholm Bay (Sweden), the Gulf of Finland, and Mecklenburg Bay (Germany) (Vanek and Lee 1991; Piekarek-Jankowska 1996; Bussmann and Suess 1998; Kaleris et al. 2002; Pempkowiak et al. 2010; Schafmeister and Darsow 2011; Virtasalo et al. 2019; Kłostowska et al. 2020; Idczak et al. 2020; von Ahn et al. 2021), but without details on possible SGD-borne nutrient loads. A well-investigated SGD location was conducted at Mittelgrund in Eckernförde Bay (Germany), where a moraine remnant intersects a confined aquifer and methane-enriched SGD emanates from the seafloor at a water depth of ~25 m, forming a pockmark morphology (Whiticar and Werner 1981; Schlüter et al. 2004; Hoffmann et al. 2020). However, no information on nutrient fluxes associated with SGD at this site has been published.

In order to investigate the SGD-borne nutrient supply to the coastal waters, we primarily studied the occurrence and magnitude of SGD along the coastline of Eckernförde Bay. This area is surrounded by agriculture associated with fertilizer usage, and therefore, is susceptible to elevated human derived nutrient fluxes toward the sea. In Kiel Bay, eutrophication-induced nitrogen limitation (N:P < 10) has been detected with a shift in phytoplankton species composition and a doubling of phytoplankton biomass within the last 100 years (Wasmund et al. 2008). Based on our surveys of the distribution of low saline pore waters and nutrient concentrations in coastal sediments, we selected four locations (Hemmelmark, Kiekut, Krusendorf, Langholz) for detailed studies, including sampling and analysis of coastal pore water, seepage meters and radium isotope mass balance models.

The Subterranean Estuary

SGD will occur whenever the hydraulic head on land is above mean sea-level and permeable pathways through lithological units connect continental aquifers to the seafloor (Johannes 1980). SGD consists of a continent-derived freshwater component (F_{SGD}) driven by the hydraulic gradient of the aquifer and a recirculated seawater component (S_{SGD}) driven by tidal pumping and wave setup, which cause seawater circulation through sediments (Santos et al. 2012; Taniguchi 2002; Burnett et al. 2006). Both components mix in the subterranean estuary (STE, Moore 1999). The classical model of a STE describes the flow of F_{SGD} towards the sea above a seawater wedge forming a fresh groundwater/seawater interface (Ghyben 1889). Density gradients along this interface cause a convective circulation. Wave-setup and tidal oscillations lead to recirculation of seawater forming an "upper saline plume" (USP) in the intertidal zone of the beach (Robinson et al. 2007a, b). Between the USP and the seawater wedge, a freshwater tube (FSP) discharges freshwater near the waterline. The occurrence and dimensions of USP and FSP depend on tidal amplitudes, ground water flux, beach slope and wave oscillations (Evans and Wilson 2016; Robinson et al. 2007a, 2007b). Geochemical reactions in the STE caused by mixing process of F_{SGD} and S_{SGD} determine the chemical composition of SGD discharging to coastal waters (Charette et al. 2005; Couturier et al. 2017; McAllister et al. 2015; Robinson et al. 2018; Moore and Joye 2021). Specifically, whether STEs are a source of nitrogen to the coastal environment may be related to both nitrogen consumption in the STE and SGD rates (Santos et al. 2008). Thus, the knowledge of the salinity-nutrient relationship in an STE is important for understanding SGD-borne nutrient fluxes.

Fig. 1 Overview map of the northern part of Kiel Bay with Eckernförde Bay located in the South-Western Baltic Sea. Four stations were studied in detail with Hemmelmark and Langholz at the northern and Kiekutt and Krusendorf along the southern coastline of Eckernförde Bay
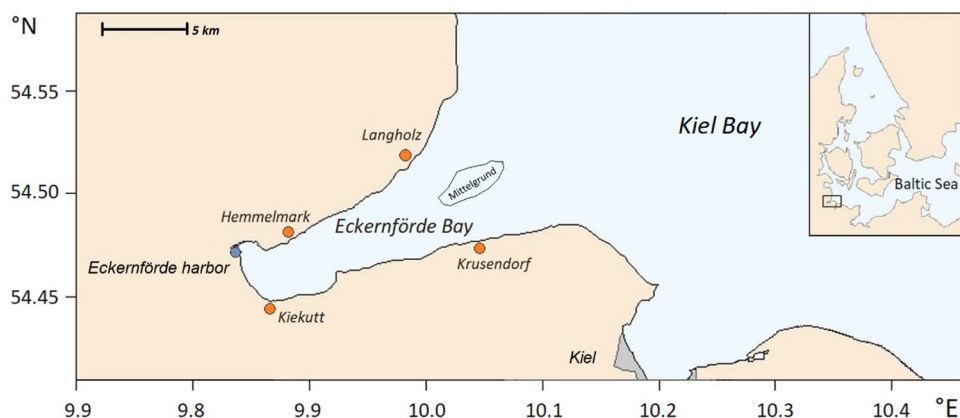
Study Area

The funnel shaped Eckernförde Bay is situated in the south-western Baltic Sea, Germany (Fig. 1). The morphology of the southwestern Baltic Sea was formed during the late Weichsel ice advances leaving a coastline of end-moraines, cliff coasts exposing till and glacial outwash sand beaches (Jensen et al. 2002). The water depth in the south-western Baltic Sea is ≤ 30 m with slopes gently rising towards the coastline. The sea level is predominantly wind controlled with little range (< 20 cm). The western Baltic Sea is characterized by a humid climate with year-around precipitation (~ 800–1000 mm per year). The coastline of Eckernförde Bay is around 40 km long and subsurface tertiary deposits as well as glacial and postglacial sediments determine the morphology of the inlet (Seibold et al. 1971). The area of the watershed around Eckernförde Bay, which is estimated to be around 150 km^2 (Marczinek and Piotrowski 2002), is defined by 50–80% agricultural land cover and is drained by a few irregularly monitored creeks (LLUR 2020).

Methods

Coastal Pore Water Sampling

In 2012, sediment pore water (~ 20–30 cm sediment depth) was collected at locations along Eckernförde Bay coastline by using a push-point piezometer (AMS™—Gas Vapor Probe System, USA, Charette and Allen 2006). Based on this survey, accessibility of the beach, and applicability of the methods used (e.g., possibility to deploy seepage meters and push-points), four locations (Hemmelmark, Langholz, Kiekut, Krusendorf) were selected for more detailed studies of the STEs and SGD (Table 1). No major streams enter these locations but heterogeneously distributed sediments with a higher amount of boulders at Kiekut and Langholz were noticed. All sampling methods were limited to the magnitudes of coastal processes like wind, waves, and currents and thus, sampling campaigns were conducted at rather calm westerly wind conditions. With the exception of Hemmelmark (see the "Results" section) negligible water level fluctuations were recorded.

Table 1 Overview of field surveys in Eckernförde Bay with dates and applied methods

Location	Latitude °N	Longitude °E	Date	Methods
Shoreline survey—Eckernförde Bay			2012–6-18, 2012–8-15	Push-point piezometer
Hemmelmark	54.4758	9.8763	2013–8-1	Push-point piezometer, seepage meter
Hemmelmark	54.4758	9.8763	2014–4-8–2014–4-16	Push-point piezometer, seepage meters, CTD-Diver, Rhizone deployments
Langholz	54.5113	9.9778	2014–6-30–2014–7-4	Push-point piezometer, seepage meters,
Krusendorf	54.4756	10.0291	2015–6-15–2015–6-20	Push-point piezometer, seepage meters
Kiekut	54.4478	9.8653	2015–9-3–2015–9-5	Push-point piezometer, seepage meters
Littorina cruise Eckernförde Bay			2016–6-7–2016-6-11	Radium water column sampling
Hemmelmark, Langholz, Kiekut	54.4759	9.8763	2016–9-26–2016-9-27	Radium push-point sampling
Hemmelmark	54.4758	9.8763	2018–23-8–2018-24-8	Radium push-point sampling, seepage meter (radium),
Hemmelmark, Langholz	54.4758 54.5113	9.8763 9.9778	2014–7-1	Helium/Tritium sampling

At Hemmelmark and Langholz, collection of sediment pore water by a push-point piezometer was performed along ~ 10 m and ~ 12.5 m cross-shore transects, covering the area from the waterline to a water depth of about 1.5 m. The horizontal and vertical sampling resolution along these transects was 1 m and 25–50 cm (± 10 cm; Charette and Allen 2006), respectively. Depending on the sediment characteristics, we were able to collect pore water from up to ~ 3 m sediment depth. At Kiekut and Krusendorf, only a few pore water samples could be obtained due to very coarse sand and gravel sediments.

Pore water (~ 200 ml) was pumped via a push-point piezometer into a beaker using a hand-held vacuum pump (Mityvac Vacuum Pump™, USA) and subsequently filtered through 0.2 µm filters (Acrodisc® Membrane Filters, 32 mm, USA). For nutrient analyses, pore water was filtered into polystyrene test tubes (volume 11 ml) and deep-frozen until further analyses. For analyses of chloride, aliquots were filled in 2 ml Eppendorf cups. Salinity, conductivity and temperature were determined in the remaining aliquot using a hand-held salinometer (WTW 3310, Germany).

Rhizon samplers (Seeberg-Elverfeldt et al. 2005) were further deployed in the STE at Hemmelmark for increased sample resolution through the salinity gradient. About 7–9 Rhizons were horizontally attached to a plastic grid, which was vertically pushed up to ~ 30 cm into the sediments. Pore water sampling started 3 days after the deployment to allow for the recovery of stable geochemical conditions. All pore water samples are categorized as STE samples, and an overview of the field surveys and methods used are summarized in Table 1.

Temporal Salinity Variations of Sediment Pore Water

In order to monitor temporal salinity variations in the sediment pore water in relation to fluctuating sea levels, a mini CTD-diver (Eijkelkamp Soil and Water, Netherlands) was deployed within sediment at depth of 20–30 cm at Hemmelmark. The CTD-Diver recorded salinity, temperature and pressure every 10 min. In addition, sea level data were collected from a nearby weather monitoring station at Eckernförde harbor (provided by Wasserstraßen- und Schifffahrtsverwaltung, www.pegelonline.wsv.de).

Helium-Tritium Sampling and Groundwater Age Dating

Samples for ^{3}H analyses were collected in 1 L plastic bottles. Samples for He isotopes and Ne analyses were collected by connecting the push-point piezometer to 40 ml copper tubes. Pumping of water was performed using a hand-held vacuum pump (Mityvac Vacuum Pump™). Note that this setup may be susceptible to degassing, which would lead to erroneous results. However, the structure of the groundwater system, did not allow another method for groundwater sampling. The copper tubes were flushed several times with groundwater before they were sealed with pinch-off clamps. Analyses of ^{3}H, He isotopes and Ne were conducted at the noble gas laboratory of the Institute of Environmental Physics, University of Bremen, Germany. A detailed description of the analytic procedure can be found in Sültenfuß et al. (2009). For groundwater samples, the precision of the He and Ne concentrations is better than 1% (Table 2). All ^{3}He components not produced by ^{3}H decay are identified via means of ^{4}He and Ne measurements. As we did not detect any terrigenic He components, we could separate the tritiogenic ^{3}He by means of ^{3}He-^{4}He ratio only, therefore, recharge conditions of the water samples need not to be accounted for. Groundwater age dating was applied using both ^{3}H and its decay product ^{3}He$_{trit}$ (Tolstikhin and Kamenskij 1969). Using the relationship between ^{3} and ^{3}He$_{trit}$ gives a time parameter, the apparent ^{3}H-^{3}He age (Eq. 1). This apparent age reflects the residence time of groundwater in the saturated zone as the elapsed time between recharge (last contact with atmosphere) and sampling. (Cook and Solomon 1997; Schlosser et al. 1988; Sültenfuß et al. 2011).

$$\tau = \frac{1}{\lambda} \cdot ln\left(1 + \frac{^3He_{trit}}{^3H}\right) \tag{1}$$

with τ = ^{3}H-^{3}He age [yrs], λ = decay constant = 0.05626 yr^{-1}, ^{3}H = concentration of ^{3}H [TU], ^{3}He$_{trit}$ = concentration of ^{3}He$_{trit}$ [TU] produced by the radioactive decay of ^{3}H.

SGD Detection via Seepage Meter Measurements

Lee-type seepage meters were used to determine the SGD rates. The devices capture SGD passing through the chemical reactor of the STE and thus enable a detailed chemical

Table 2 Ages of sediment pore waters from the STE at Hemmelmark and Langholz determined by the Helium/Tritium method. Tritium concentrations and ages are scaled to 1st of July 2014

Location	Salinity	Sediment depth (cm)	Water depth (cm)	Tritium [TU]	He/T ages (years)
Hemmelmark	0.3	60	50	5.5 ± 0.1	11 ± 2
Hemmelmark	0.3	240	50	5.1 ± 0.1	19 ± 2
Langholz	0.3	100	15	4.4 ± 0.1	no data
Langholz	0.3	200	15	± 0.1	39 ± 2

characterization of SGD, determination of discharging rates as well as variations over tidal cycles (Lee 1977; Taniguchi 2002). Seepage meters may suffer from sampling artefacts in case of low seepage rates (< 12 cm d^{-1}) and strong waves (Russoniello and Michael 2015; Shaw and Prepas 1989). Seepage meters inherently cover only a small area of the seafloor (typically 0.25 m^2), therefore, many measurements (spots) are necessary to derive spatially and temporally representative seepage rates. Our 4 seepage meters were deployed 50 m apart of each other along the beaches. After ~ 2 days all seepage meters were moved 2 m offshore from the same station. A total of 361 seepage meter measurements were conducted with $n = 174$ at Hemmelmark, $n = 82$ at Langholz, $n = 86$ at Krusendorf and $n = 19$ at Kiekut. Due to microtidal conditions, the tidal cycle was not considered.

In order to collect SGD waters, we attached a plastic bag (10 L) to the outlet on top of the seepage meter. The deployment time of the bags was between 15 and 60 min. Thereafter, the water volume in the bag was measured through a volumetric flask, and salinity and temperature were determined through a hand-held WTW-Salinometer. Deployments of seepage meters were limited to water depths of 30–130 cm in areas characterized by sandy sediments, and were conducted along cross-shore transects at Hemmelmark, Langholz, Kiekut, and Krusendorf. Filtered nutrient samples were obtained after seepage meters were completely flushed with SGD, which was indicated by a constant salinity over several consecutive deployments. The SGD rates (F) were calculated as follows (Burnett et al. 2001) and expressed as a flow velocity:

$$F\left[cm\ d^{-1}\right] = \frac{V}{T} * \frac{1440}{A} \qquad (2)$$

with V = water volume in the bag [cm^3]; T = time the bag was attached to the seepage meter [min]; A = the surface area of the seepage meter (2560 cm^2). Freshwater SGD flux (F$_{SGD}$) was determined after seepage meters were completely flushed and calculated as follows:

$$F_{SGD}\left[cm\ d^{-1}\right] = \frac{SalSW - SalSP}{SalSW} * F \qquad (3)$$

Sal$_{SW}$ is the ambient seawater salinity, Sal$_{SP}$ is the salinity of the water in the seepage meter and F (cm d^{-1}) is the total seepage meter water flux.

Radium Isotope Measurements

A spatial and temporal integration of SGD is possible through the application of radium isotope mass balances (Moore 2003, 2006). Radium (Ra in the following) isotopes, such as ^{224}Ra (t$_{1/2}$ = 3.7 d) and ^{223}Ra (t$_{1/2}$ = 11.5 d), are produced by radioactive decay of thorium, which is ubiquitous in sediments and rocks. Whereas Ra is not mobile in freshwater, it is released from sediments in the STE at salinities of ~ 3–4, and subsequently cause SGD to be enriched in Ra relative to seawater. Through mass balance models of Ra, which consider all sources and sinks of Ra in the coastal ocean, a spatially and temporally integrating measure of SGD can be obtained (Moore 2000, 2003; Garcia-Orellana et al. 2021).

We collected about ~ 100 L of seawater per sample during a R/V Littorina research cruise (L16/09, 7–11 June 2016) in Eckernförde Bay. Upon collection, water samples were passed at a flow rate of about 1 L min^{-1} through a column filled with 20 g of manganese-coated acrylic fiber (MnO$_2$ fiber) to adsorb Ra onto the MnO$_2$ fibers. The Ra-loaded MnO$_2$ fibers were then rinsed with Ra-free water to remove sea salt and partially dried. A push-point piezometer was used to sample sediment pore water for Ra endmembers within the STE´s of Hemmelmark, Kiekut and Langholz. About 2.5–4 L of pore water was extracted and poured over MnO$_2$ fibers. In addition, water samples for salinity and nutrient analyses (selected) were obtained from both surface and pore waters. Furthermore, a 5L water sample for Ra determination was obtained by seepage meter at Hemmelmark.

Partially dried MnO$_2$ fibers were placed in a Radium Delayed Coincidence Counter (RaDeCC) system (Moore and Arnold 1996) following the measurement procedure outlined in Moore et al. (2008). The ^{228}Th activity was measured 3 weeks after the first measurement of ^{224}Ra, when the initial ^{224}Ra has decayed and the supported ^{224}Ra has equilibrated with its parent ^{228}Th adsorbed onto MnO$_2$ fiber. Excess ^{224}Ra (^{224}Ra$_{ex}$) was calculated by subtracting the ^{228}Th activity from the ^{224}Ra activity. The RaDeCC efficiency for ^{224}Ra measurements was determined by using an IAEA reference source (Scholten et al. 2010); whereas the ^{223}Ra efficiency was calculated following the method of Moore and Cai (2013). Uncertainties of measurements were propagated according to Garcia-Solsona et al. (2008). The analytical precision of Ra analysis by RaDeCC was 7–10% in our measurements.

Radium Mass Balance Model for SGD Estimations

We used a ^{224}Ra$_{ex}$ mass balance model for SGD estimations, which assumes steady state between all sources and sinks of ^{224}Ra$_{ex}$ (Beck et al. 2007; Krall et al. 2017; Moore 2000; Garcia-Orellana et al. 2021).

$$J_{Sea} + J_{Decay} = J_{Diff} + J_{SGD} + J_{Riv} \qquad (4)$$

where J_{Sea} is the ^{224}Ra$_{ex}$ flux exported from the areas investigated to the bay, J_{Decay} is the loss of ^{224}Ra due to radioactive decay, J_{Diff} is the ^{224}Ra$_{ex}$ flux resulting from Ra diffusion from sediments, J_{SGD} is ^{224}Ra$_{ex}$ supplied via SGD

and J_{Riv} is the river $^{224}Ra_{ex}$ flux. As there are no rivers draining into Eckernförde Bay J_{Riv} was omitted.

J_{Sea} was determined through the $^{224}Ra_{ex}$ excess inventory (I_{ex}, i.e,. total $^{224}Ra_{ex}$ inventory in the investigated areas in excess of the $^{224}Ra_{ex}$ supplied by open bay waters) divided by the residence time (τ) of waters in the investigated areas. This residence time was calculated as following Moore (2006):

$$\tau = ln\left(\frac{AR_i}{AR_{obs}}\right)\frac{1}{\lambda_{224} - \lambda_{223}} \qquad (5)$$

with AR_i and AR_{obs} are the average measured and the initial (endmember) $^{224}Ra_{ex}/^{223}Ra$ activity ratios, λ_{224} and λ_{223} are the decay constants of $^{224}Ra_{ex}$ and ^{223}Ra, respectively. The loss of $^{224}Ra_{ex}$ derived by radioactive decay (J_{Decay}) was calculated by multiplying the $^{224}Ra_{ex}$ activities measured along each cross-shore transects with the respective water depths and averaging the results. This average inventory (I) was multiplied by the surface area (A [m^2]) of the specific area investigated and by the ^{224}Ra decay constant (λ).

Thus:

$$J_{SGD} = J_{Diff} * A + \frac{I_{ex}}{\tau} - I * \lambda \qquad (6)$$

The volume of SGD flux (cm d^{-1}) was determined by dividing J_{SGD} (dpm d^{-1}) by the endmember $^{224}Ra_{ex}$ activities (dpm m^{-3}) and by the surface area of the investigated location.

Nutrient Analysis

Water samples for nutrient analysis were deep-frozen at -20 °C until analysis. Nutrient concentrations were analyzed by a QuAAtro39 Auto Analyzer of Seal Analytics at the Alfred- Wegener Institute, Bremerhaven. The device is an automated Continuous Segment Flow Analyzer (CFSA) and allows quantitative determinations of ammonia, nitrate and nitrite, and phosphate. In total, 171 samples were analyzed (Hemmelmark: $n = 53$; Langholz: $n = 37$; Krusendorf: $n = 40$; Kiekut $n = 41$). According to the European Protection Agency (EPA), method detection limit (MDL) for DIN ($NH_4^+ + NO_2^- + NO_3^-$) is 0.01 µmol L^{-1} (Kérouel and Aminot 1997) with a standard deviation (SD) of 0.027 µmol L^{-1}. The determination of PO_4^{3-} is based on the colorimetric *Method No. Q-064–05 Rev. 4 (Royal Netherlands Institute for Sea Research, NIOZ)*. MDL and SD for PO_4^{3-} are 0.01 µmol L^{-1} and 0.061 µmol L^{-1} (acc. EPA), respectively (NIOZ).

Results

Pore Water Salinities in the Coastal Sediments

A survey along the coastline of Eckernförde Bay in 2013 revealed a widespread occurrence of low-salinity pore waters. Low salinity ratios of ≤ 0.75 (pore water to surface seawater) were detected at 19 out of 23 stations investigated (Fig. 2). The lowest salinity ratios of ≤ 0.08 characterized by pore water salinities of ≤ 0.3 were observed at seven locations irregularly distributed around the coastline of Eckernförde Bay.
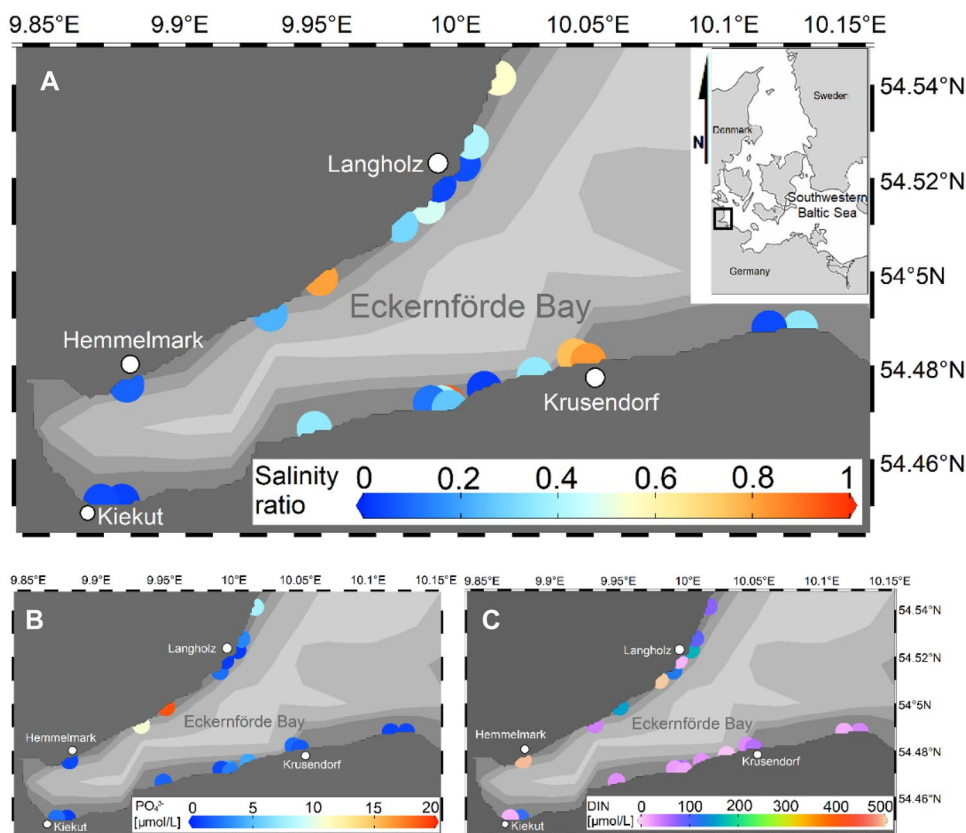
The pore-water transects at Langholz (Fig. 3A) and Hemmelmark (Fig. 3B) revealed a clear extension of a low-salinity aquifer into the submarine sediments. For both locations, surface water salinities ranged between 15.7 and 19.8. Along the transect in Langholz, pore water salinities of < 1 were predominantly found at sediment depths of > 80 cm near the shoreline; while at the end of the transect, lower salinities were observed only at a greater sediment depth of > 1.60 m (Fig. 3A). In between these sampling points, variable salinities on horizontal as well as vertical scales occurred reflecting a complex mixing between low saline groundwater and surface seawater. At Hemmelmark, a steep salinity gradient in the submarine surface sediments was observed with salinities ≤ 0.3 prevailing below ~ 50 cm sediment depth. This gradient was detected across the complete cross-shore transect.

Pore water derived from Rhizones at Hemmelmark revealed a strong decrease in salinities within sediment depths between 6 cm (salinity 17) and 10 cm (salinity < 0.3) (Fig. 4). In contrast, two profiles of 2014/04/14 and 2014/04/15 showed increasing DIN concentration below sediment depth of 6 cm. For profile of 2014/04/15, salinity indicated a smaller gradient across the sediment column (salinity of ~ 10 below 10 cm sediment depth), but this gradient got relatively steep in the following day.

Relation of Pore Water Salinities and Sea Level

In order to investigate the fluctuations of salinity in pore waters, a MiniCTD diver was deployed for 9 days at Hemmelmark next to the Rhizon pore water samplers (Fig. 5, see Fig. 3 for the location of deployment). During this deployment period, seawater salinities varied between 16.3 and 19.6, and sea level fluctuations of up to 70 cm were recorded. A significant correlation between seawater level and salinities ($r^2 = 0.68$, $p < 0.001$, $n = 2054$) was found. Some of these variations are caused by micro tides (e.g., period 2014/4/11–2014/4/13, Fig. 5), as indicated by a 6 h sea level cycle. During days of stronger west and southwesterly winds (e.g., period 2014/4/13–2014/4/15), low sea level is accompanied by nearly constant and low sediment pore water salinities. A decrease in the wind strength (e.g., on 2014/4/15) causes higher sea level (2014/4/10, 2014/4/15–2014/4/16) with increasing pore water salinities (> 15). However, a time lag between sea level fluctuation and pore water salinity can be observed.

Fig. 2 Eckernförde Bay with locations of a coastal SGD surveys. The insert in A) shows the location of Eckernförde Bay in the southwestern Baltic Sea. **A** Salinity ratios of surface sediment pore water and ambient seawater; **B** phosphate (PO_4^{3-}) concentrations in pore water; **C** pore water dissolved total inorganic nitrogen ($DIN = NH_4^+ + NO_2^- + NO_3^-$) concentrations. Langholz, Hemmelmark, Kiekut, and Krusendorf are the location where depth profile studies were conducted

Helium/Tritium Ages of Pore Water in Coastal Sediments

At the reference points of all the cross-shore transects at Langholz and Hemmelmark (see Fig. 3A, B), pore water samples were obtained (Table 2) for Helium/tritium age analysis. At Hemmelmark, the apparent ages of pore water collected at two different sediment depths were 11 ± 2 and 19 ± 2 years. However, the highest age of 39 ± 2 years was observed in 200 cm sediment depth at Langholz. A shallow pore water sample from the same site was contaminated with atmospheric air, and thus could not be used to derive tritiogenic ^{3}He, hence an age could not be calculated.

SGD Rates

Seepage Meters

A total of 361 seepage meter measurements were conducted throughout the sampling campaign with an overall mean SGD rate of 21.6 ± 25 cm d^{-1} (range 0.6–173 cm d^{-1}). Most of the measured SGD rates ($n = 258$) were < 20 cm d^{-1}. Only two measurements revealed SGD rates > 150 cm d^{-1} (Fig. 6A). The mean SGD rates at Hemmelmark, Langholz, Krusendorf, and Kiekut were 18.8 ± 16 cm d^{-1} (range 0.5–80 cm d^{-1}, $n = 174$), 33.3 ± 42.7 cm d^{-1} (range 1.6–173 cm d^{-1}, $n = 82$), 11.6 ± 5.3 cm d^{-1} (range:

2.6–29.3 cm d^{-1}, $n = 86$) and 21.6 ± 22.3 cm d^{-1} (range: 0.8–128 cm d^{-1}, n = 19), respectively. For Hemmelmark, Langholz and Krusendorf, the fraction of F_{SGD} (Eq. 3) was 14.6%, 14.5%, and 21.4%, respectively (Fig. 6B), but seepage meter measurements at Kiekut did not reveal any detectable F_{SGD} fraction (Fig. 6B). SGD rates > 100 cm d^{-1} were observed at locations with water depths of < 60 cm and the highest SGD rates (> 150 cm d^{-1}) at locations where water depth is < 45 cm. At the locations with water depth of > 100 cm, SGD rates decreased below 11 cm d^{-1}. SGD rates in the range of the mean values prevailed at the locations with water depths of < 80 cm (Fig. 6C).

Radium Mass Balance Model

In surface waters at the locations investigated, we observed decreasing ^{224}Ra$_{ex}$ with increasing distance to the shore (Fig. 7). The average ^{224}Ra$_{ex}$/^{223}Ra ratios (AR$_{obs}$) along these transects were 13.1 ± 4.78, 13.0 ± 4.35, and 13.1 ± 3.4 at Hemmelmark, Langholz and Kiekut, respectively. Based on the endmembers collected in the areas investigated and characterized by salinities > 3 (Table 3), we calculated average residences times (Eq. 5) of 5.0 ± 1.8 days for Langholz, 5.5 ± 2.3 days for Hemmelmark, and 4.5 ± 1.5 days for Kiekut. For calculating the ^{224}Ra$_{ex}$ flux resulted from diffusion from the sediments (J$_{Diff}$), we used a benthic ^{224}Ra$_{ex}$ flux
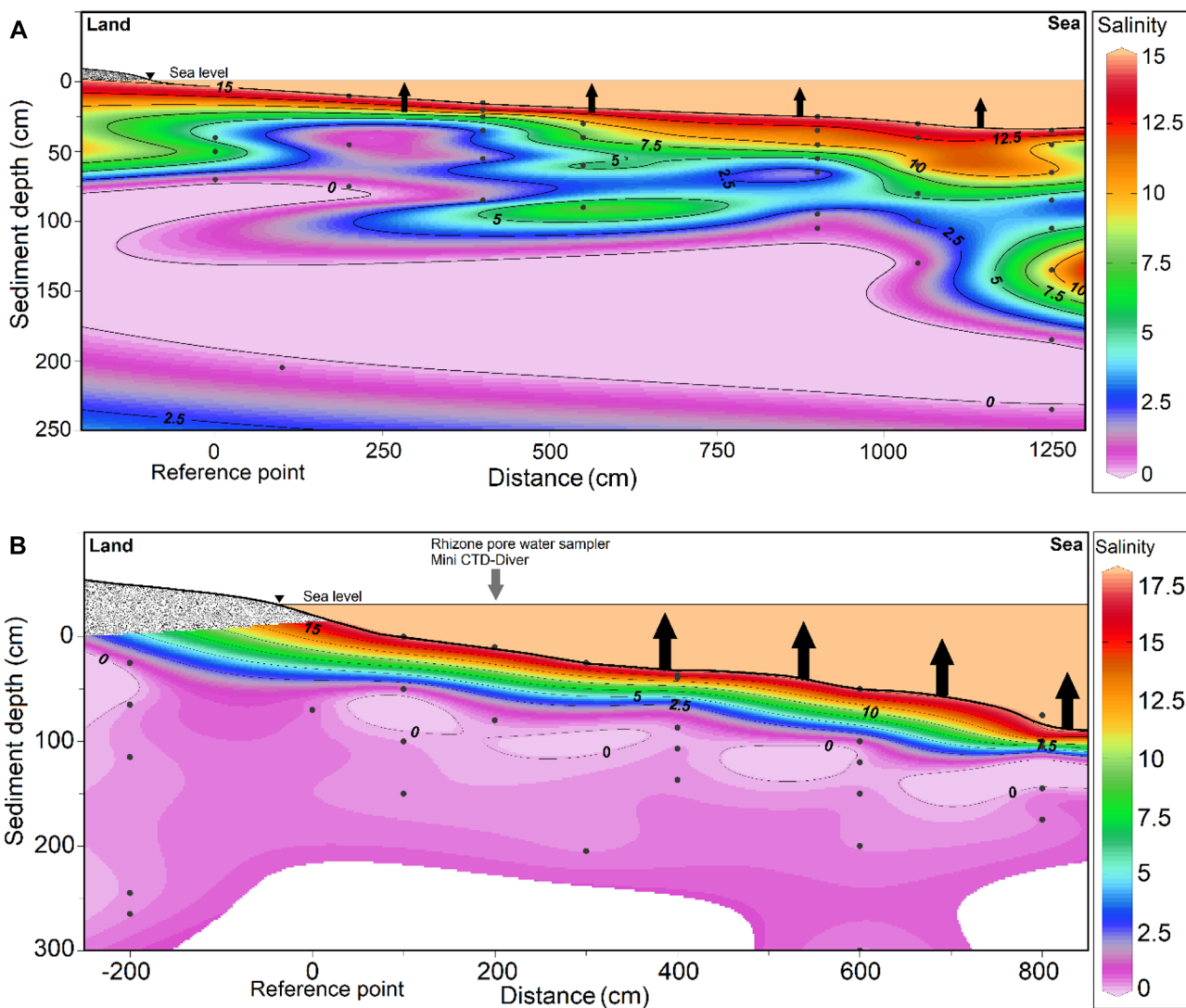
Fig. 3 Cross-shore transects of salinity distributions in the STEs of **A** Langholz and **B** Hemmelmark (*Ocean Data View, Version 5.2.0);* and. The black dots indicate the sampling locations of pore water.

The black arrows show the locations of seepage meter deployed; the gray arrow in **B** marks the positions of Rhizone sampling and Mini CTD-Diver deployment

(F_{diff}) of 31.6 ± 1.8 dpm m^{-2} d^{-1} determined by Krall et al. (2017) for Baltic Sea sediments, and assumed that this flux is also characteristic for the area investigated. Based on the

^{224}Ra$_{ex}$ mass balance model (Eq. 6), we calculated SGD rates of 15.4 ± 5.4 cm d^{-1} at Hemmelmark, 23.3 ± 5.8 cm d^{-1} at Langholz and 1.23 ± 0.4 cm d^{-1} at Kiekut. These estimates

Fig. 4 Salinity (green) and dissolved inorganic nitrogen concentrations (orange dots, 2014/04/14, 2014/04/15) profiles obtained from the STE at Hemmelmark using Rhizon pore water samplers, and where steep salinity gradients in shallow sediments could be observed
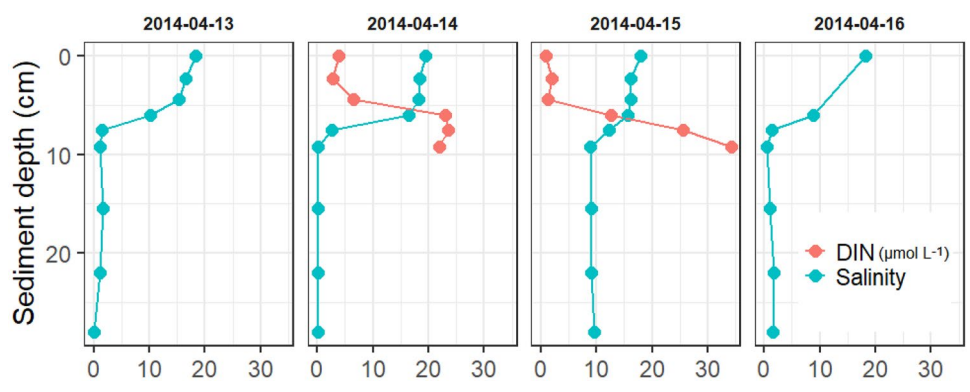
Fig. 5 The upper graph shows sea level data [cm] retrieved from the gage station located in the harbor of Eckernförde (see Fig. 1). The sea level data is provided by Wasserstraßen-/ Schifffahrtsverwaltung (www.pegelonline.wsv.de) and refers to standard elevation zero (NHN), being − 5.003 m at this location. Mean sea level for the time period of Nov 2005 to Oct 2015 is 504 cm, indicating various events with elevated sea level situations. The graph in the middle represents pressure [mbar] that was recorded by the buried conductivity-, temperature-, depth sensor (Schlumberger Mini CTD-Diver) and reveals a representation of the water fluctuation at the site with salinity (lower graph) over time. The CTD-Diver was buried at sediment depth of ~25 cm in the submerged sediments close to the waterline (see Fig. 3B) from the 2014/04/09 until 2014/04/17
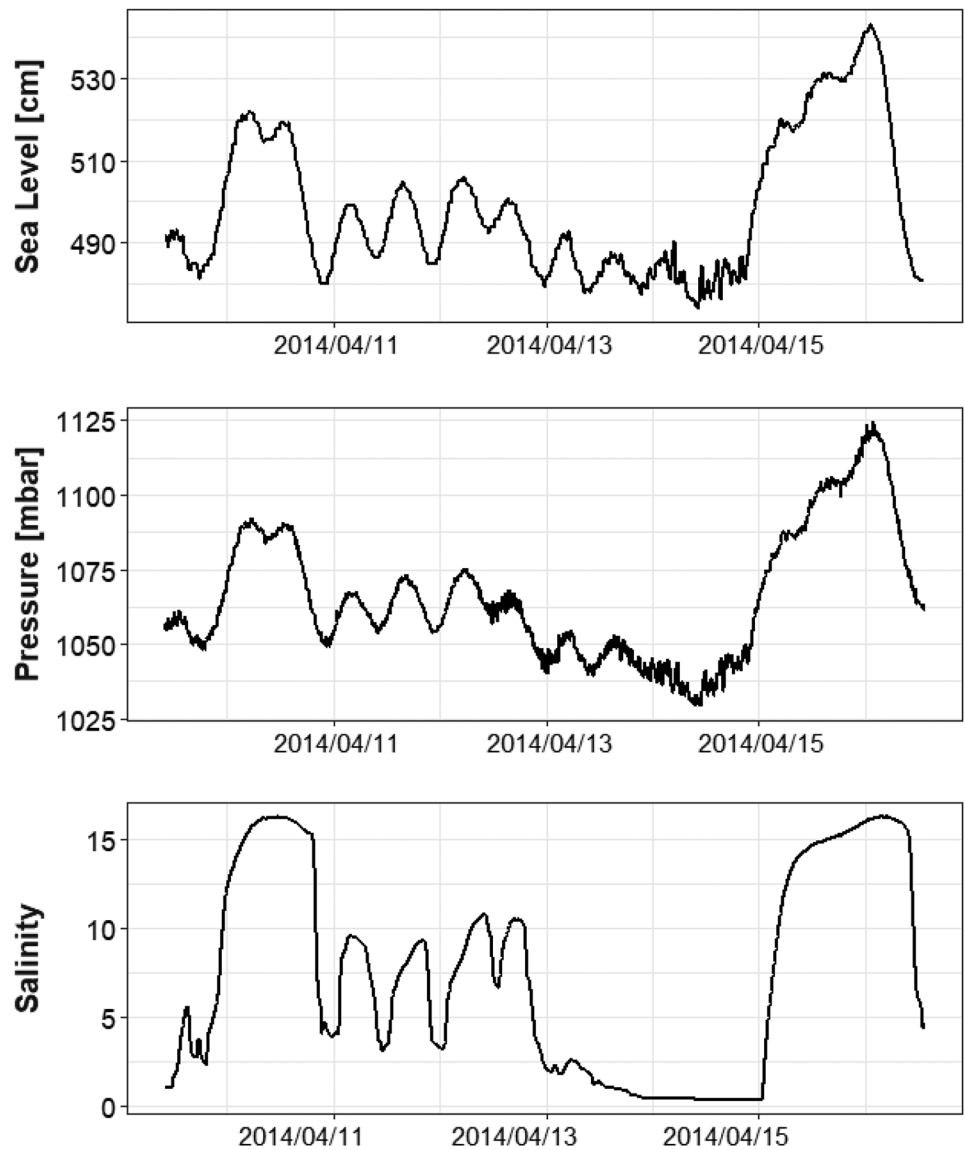
agree well with those derived from seepage meter except for Kiekut, where Ra-based SGD rates exhibited lower. The SGD rates reported by Schlüter et al. (2004) for the entire seabed of Eckernförde Bay (70 km^2) are based on freshwater flow from sub seafloor aquifers using ^{222}Rn measurements and are significantly lower (0.015–0.2 cm d^{-1}) than our results.
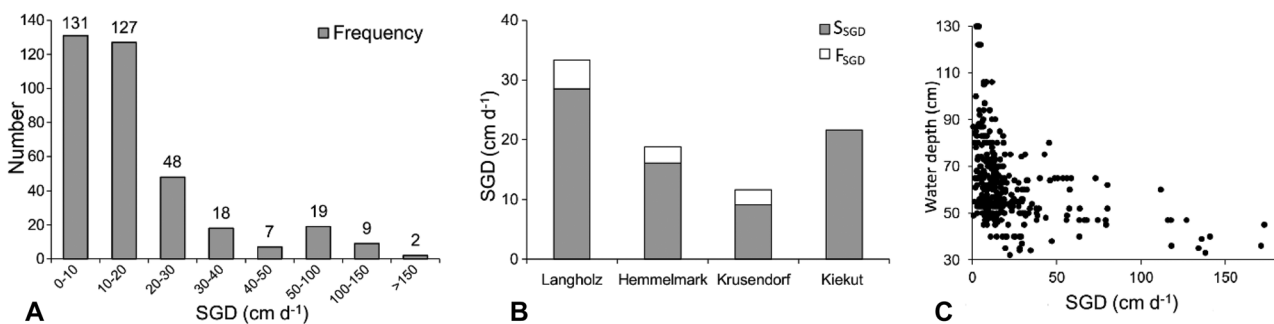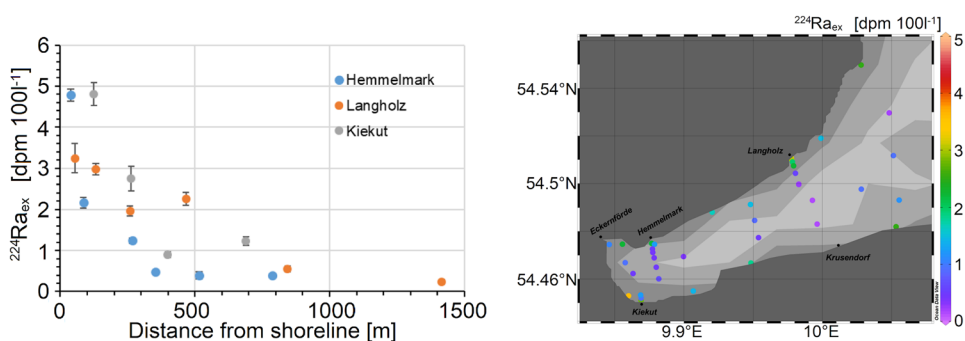

Fig. 6 **A** Frequency of SGD rates, **B** mean SGD rates (cm d^{-1}) for fresh (F$_{SGD}$) (except Kiekut) and recirculated S$_{SGD}$, **C** relation between SGD flux and water level indicate increasing SGD rates with decreasing water level

Fig. 7 Left: cross-shore $^{224}Ra_{ex}$ activities at Hemmelmark, Langholz and Kiekut; Right: $^{224}Ra_{ex}$ activities in surface waters of Eckernförde Bay

Nutrients

Nutrient Distribution in STEs

Dissolved inorganic nitrogen concentrations (DIN = NH_4^+ + NO_2^- + NO_3^-) in pore waters along the coastline of Eckernförde Bay revealed a strong heterogeneity during the 2012 survey (Fig. 2) with mean DIN concentrations of 92.6 ± 135 µmol L^{-1} (range: 1.6–496 µmol L^{-1}; $n = 23$) and mean PO_4^{3-} concentrations of 3.3 ± 4.4 µmol L^{-1} (range: 0.36–18.9 µmol L^{-1}; $n = 21$). Highest DIN concentrations (496 µmol L^{-1}) and PO_4^{3-} (18.9 µmol L^{-1}) were found at Hemmelmark. In general, pore waters from the northern shoreline exhibited fivefold higher mean DIN (183 ± 185 µmol L^{-1}, $n = 9$) and twofold higher PO_4^{3-} (5.50 ± 6.60, $n = 8$) concentrations as compared to those concentrations along the southern shoreline (mean DIN: 34.4 ± 27.7 µmol L^{-1}; mean PO_4^{3-}: 2.0 ± 1.2 µmol L^{-1}; $n = 14$).

Nutrient-Salinity Relations in STEs

Along the salinity gradients within the investigated STEs, we observed a large range in nutrient concentrations (DIN, mean: 105 ± 195 µmol L^{-1}, range: 0.05–1.722 µmol L^{-1} $n = 173$, NH_4^+, mean: 86.6 ± 191 µmol L^{-1}, range: 0.13–1.707 µmol L^{-1}, $n = 169$, NO_2^-, mean: 0.72 ± 1.88 µmol L^{-1}, range: 0.05–12.1 µmol L^{-1}, $n = 146$, NO_3^-, mean: 21.5 ± 61.8 µmol L^{-1}, range: 0.08–493 µmol L^{-1}, PO_4^{3-}, mean: 5.32 ± 11.2 µmol L^{-1}, range: 0.03–70.5 µmol L^{-1}, $n = 169$; (Fig. 8, refer to supplementary information Tab. S2 as well). Nutrient concentrations tended to decrease with increasing salinities except at Kiekut (nutrients here remain relatively constant). In low saline pore waters (salinity ≤ 1), mean DIN and PO_4^{3-} were 59.1 ± 68.3 µmol L^{-1} (range: 7.0–289 µmol L^{-1}, $n = 24$) and 1.23 ± 1.89 µmol L^1 (range: 0.03–9.15, $n = 23$), respectively. In saline pore waters (salinity > 1), we observed a higher mean DIN of 113 ± 207 µmol L^{-1} (range: 0.05–1.722 µmol L^{-1}, $n = 149$) and a higher

Table 3 Results of ^{223}Ra, ^{224}Ra and $^{224}Ra/^{223}Ra$ activities in pore water samples collected at Hemmelmark, Langholz and Kiekut

Sample ID	Sediment depth (cm)	Salinity	^{223}Ra (dpm 100L^{-1})	^{224}Ra (dpm 100L^{-1})	Activity ratio $^{224}Ra/^{223}Ra$
Hemmelmark					
H0916-1	70	0.3	4.55 ± 0.91	92.8 ± 4.89	20.4 ± 4.21
H0916-3	40	0.1	0.34 ± 0.09	10.8 ± 0.51	31.6 ± 8.03
HEM 7.18–3	19	4.1	9.31 ± 1.59	219 ± 11.3	23.5 ± 4.19
HEM 7.18–5	8	8.7	17.3 ± 1.50	364 ± 16.4	21.0 ± 2.05
Seepage meter	-	10.6	5.35 ± 0.57	142 ± 6.09	26.6 ± 3.05
Endmember (salinity > 3)	-	-	10.7 ± 0.75	242 ± 113	22.7 ± 1.73
Langholz					
L0916-1	40	0.5	2.31 ± 0.6	47.3 ± 1.92	20.5 ± 5.39
L0916-3	20	4.7	20.0 ± 2.0	454 ± 23.2	22.7 ± 2.75
Endmember (salinity > 3)	-	-	20.0 ± 2.0	454 ± 23.2	22.7 ± 2.75
Kiekut					
K0916-1	30	16.3	11.5 ± 1.63	281 ± 9.68	24.5 ± 3.58
K0916-3	65	13.4	21.2 ± 2.02	433 ± 16.2	20.5 ± 2.10
Endmember (salinity > 3)			16.3 ± 1.14	357 ± 108	21.9 ± 3.03

mean PO_4^{3-} (5.97 ± 11.9 µmol L^{-1}, range: 0.03–70.5 µmol L^{-1}, $n = 146$). On average, the low salinity (< 1) pore water DIN and PO_4^{3-} concentrations accounts for about 60% and 30%, respectively, as in high salinity (> 1) pore waters.

Nutrient Fluxes Derived From Seepage Meters and Radium Mass Balance Model

The nutrient fluxes based on SGD rates derived from seepage meter measurements for the four investigated locations are summarized in Table 4. Highest DIN and PO_4^{3-} fluxes were observed at Langholz; whereas at the other locations, nutrient fluxes were in a similar range and comparable. The mean DIN flux for all locations were 7.94 ± 9.3 mmol m^{-2} d^{-1} (range: 0.5–18.9 mmol m^{-2} d^{-1}) and 0.4 ± 0.4 mmol m^{-2} d^{-1} (range: 0.04–1.1 mmol m^{-2} d^{-1}) for PO_4^{3-}.

For calculations of SGD nutrient fluxes, the Ra-based SGD flux must be multiplied by an endmember nutrient concentration. Here, we used two types of endmembers. First, we have chosen the range of nutrient concentrations in pore waters corresponding to the salinity range observed in the seepage meters at the locations investigated (Tab. S2). This approach assumes that salinity of SGD is a tracer for defining nutrient endmember concentrations. Second, we used the range of nutrient concentrations observed in pore waters with salinity ≤ 1. Both approaches show wide ranges of mean nutrient

fluxes (Table 4) with higher mean DIN (18.7 ± 27.4 mmol m^{-2} d^{-1}) and PO_4^{3-} (1.48 ± 2.7 mmol m^{-2} d) fluxes for the salinity range 8.4–16.3 as compared to salinity range < 1 (DIN: 9.5 ± 11.2 mmol m^{-2} d; PO_4^{3-}: 0.12 ± 0.07 mmol m^{-2} d^{-1}; Table 4). In general, nutrients fluxes based on seepage meter measurements and radium mass balances agree within a factor of ~ 2 (DIN) and 10 (PO_4^{3-}).

Discussion

We observed a frequent occurrence of low saline (≤ 1) pore waters in surface sediments along Eckernförde Bay coastline associated with DIN concentrations of up to ~ 500 µmol L^{-1} (Fig. 2). The relatively young He/T ages of these waters, ranging between 11 ± 2 years and 39 ± 2 years (Table 2), suggested their relatively recent formation, most likely related to groundwater associated with an upper unconfined aquifer present in the catchment area of Eckernförde Bay. Here, groundwater found within 1 m to 4 m below ground surface is transported along topographic gradients towards the coast (Marczinek and Piotrowski 2002). The close connection of the aquifer to the ground surface characterized by high agricultural activities causes nitrate concentrations in groundwater of up to 1290 µmol L^{-1} (Jensen et al. 2002; Marczinek and Piotrowski 2002). Groundwater recharge rates of the

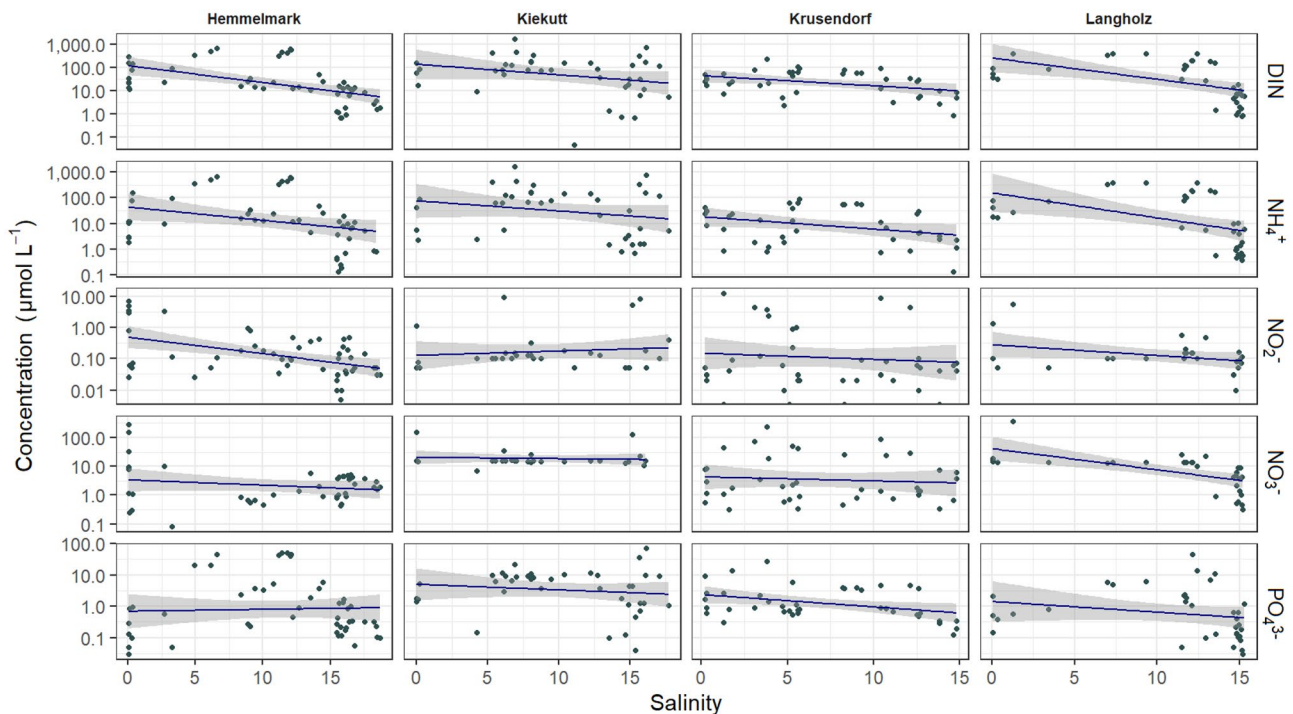**Fig. 8** Pore water concentrations (logarithmic scale) of DIN, NH$_4^+$, NO$_2^-$, NO$_3^-$ and PO$_4^{3-}$ versus salinity for samples collected at Hemmelmark, Kiekut, Krusendorf and Langholz. The solid blue lines (regression lines) and gray shadows (standard deviation) show an overall negative slope but no robust linear relationship between nutrient concentrations and salinity

Table 4 Nutrient fluxes (in mmol m^{-2} d^{-1}) for DIN and PO$_4^{3-}$ for the locations Hemmelmark, Krusendorf, Langholz and Kiekut based on seepage meter measurements (A) and a radium mass balance (B)

	Hemmelmark		Krusendorf		Langholz		Kiekut		Mean[a]	
A)	DIN	PO$_4^{3-}$	DIN	PO$_4^{3-}$	DIN	PO$_4^{3-}$	DIN	PO$_4^{3-}$	DIN	PO$_4^{3-}$
Seepage meter flux	8.9–16.3		9.0–14.8		11.7–14.6		16.0–16.3		8.9–16.3	
mean	5.1	0.89	2.93	0.16	63.1	1.61	4.4	0.09	7.94	0.48
±σ	1.99	0.60	3.26	0.18	87.94	2.22	7.6	0.10	9.32	0.44
N	9	9	14	14	2	2	4	4	29	29
min	1.34	0.09	0.24	0.02	0.11	0.04	0.1	0.01	0.52	0.04
max	7.83	1.92	11.68	0.54	125.28	3.18	15.8	0.20	18.9	1.10
B) Radium										
S range[b]	8.9–16.3				11.7–14.6		16.0–16.3		8.4–16.3	
mean	13.0	1.22			30.4	1.77	1.87	0.19	18.7	1.48
±σ	28.2	2.55			27.8	3.16	1.98	0.22	27.4	2.68
N[c]	27	27			11	11	3	3	41	41
min	0.10	0.01			0.35	0.01	0.15	0.02	0.17	0.02
max	99.9	8.01			92.9	10.7	4.04	0.44	91.0	8.18
B) Radium										
S range	<1				<1		<1		<1	
mean	13.5	0.05			11.2	0.16	0.59	0.03	9.50	0.12
±σ	14.7	0.06			15.1	0.19	0.79	0.02	11.2	0.07
N[c]	9	9			5	5	5	5	19	19
min	0.33	0.00			2.17	0.04	0.11	0.02	0.76	0.05
max	67.5	0.15			38.0	0.49	2.00	0.63	39.6	0.36

[a] weighted average

[b] Salinity range from which nutrient concentrations were chosen

[c] Number of nutrient measurements in the salinity range

watershed are estimated at 150–250 mm/a (Renger and Wessolek 1990) and shallow aquifers have typically higher rates of recharge (1–30 cm yr^{-1}) and groundwater flow velocities (1–100 m yr^{-1}) than deep aquifers (intermediate or regional flow system) with lower rates of recharge (0.01–1 cm yr^{-1}) and lower groundwater flow velocities (0.1–1 m yr^{-1}) (Slomp and Van Cappellen 2004). Coastal aquifers reach horizontal seaward flow velocities of 2–300 m d^{-1} predominantly outcropping at seepage faces such as permeable coastal sediments (Santos et al. 2011). While the measured groundwater ages agree well with the theoretical flow rates, a robust correlation with SGD rates was not found due to likely more complex driver interactions. SGD is mainly driven by complex hydrological characteristics of coastal aquifers and surface water conditions, like the groundwater recharge rates, permeability of the aquifer and the hydraulic gradients resulting in its specific groundwater discharge rates (Anderson Jr and Emanuel 2010; Gonneea et al. 2013; Luijendijk et al. 2020).

As the water table of this aquifer and the flow of groundwater are relatively constant during all the seasons, oscillation of seawater through the sediment bed in the coastal area forced by sea level fluctuations and waves is assumed to be the main driver for changes of the hydraulic gradients and thus for the groundwater flow to Eckernförde Bay. This is reflected in our time series measurements of sediment pore water salinities (Fig. 5) with low salinities during times of low sea level, translating to a higher hydraulic gradient, and therefore higher influence of fresh groundwater, and vice versa (see Temporal Salinity Variations of Sediment Pore Water). In addition, the seepage meter measurements detected opposing trends between SGD flux rates and variable water depths likely driven by variable hydraulic gradients (Fig. 6). The relatively high F$_{SGD}$ fraction of up to ~21% (SGD Detection via Seepage Meter Measurements) indicated the general importance of fresh groundwater for SGD along Eckernförde Bay.

In the following section, we will first discuss fresh groundwater–seawater mixing in the STEs of Hemmelmark and Langholz. Second, we will discuss the nutrient distributions along the salinity gradients in STEs and the results of SGD nutrient fluxes to Eckernförde Bay.

The STEs at Hemmelmark and Langholz

Compared to the established concepts of STEs, there are three apparent differences in the structure of the STEs observed at Hemmelmark and Langholz. First, we do not find the typical saltwater wedge in the STE, which normally extends from below the groundwater to the open sea (Fig. 3). One likely explanation is that our vertical and lateral sampling scheme does not cover the full dimensions of the studied STEs.

Second, we do not observe a distinct USP, a seawater circulation cell in the intertidal zone mainly driven by the tidal range and wave set-up (Robinson et al. 2007a, b; 2018). The Baltic Sea has a microtidal environment (tidal range < 20 cm) and the locations investigated were not exposed to waves higher 30 cm (Langholz ~ 30 cm; Hemmelmark ~ 10 cm) during the sampling campaigns. Therefore, the necessary requirements for a development of an USP seems to be lacking. Instead, we observe a strong vertical density gradient (Figs. 3 and 4) with heavier saline seawater overlaying fresh groundwater. The steep density gradient indicates a relatively strong upward advection of fresh groundwater, which limits density driven downward mixing of seawater, like the development of salt fingers that circulate into the groundwater (Breier et al. 2005; Rapaglia and Bolunewicz 2009; Greskowiak 2014; Röper et al. 2015). Compared to Hemmelmark, we observed some undulations of the freshwater/seawater gradient in the STE of Langholz (Fig. 3), Langholz is characterized by a gentler beach slope and is more exposed to the open bay so that wave activity may have some influence on seawater/groundwater mixing here. Third, we do not observe a direct discharge of F_{SGD} normally characterizing a freshwater tube (FDT) of STE's. In our study, a fresh groundwater layer is horizontally orientated and does not outcrop at the seafloor. One reason may be that the occurrence of a FDT is closely linked to the USP (Evans and Wilson 2016; Robinson et al. 2007a). The lack of a USP might also be the reason why the composition of our SGD is characterized by a relatively high F_{SGD} fraction (mean F_{SGD} ~ 17%). In other SGD systems studied worldwide, tidal-pumping and wave set-up are the most important drivers for SGD and the recirculation of seawater through the STE results in F_{SGD} fractions in the range of around 5–10% (Burnett et al. 2006; Taniguchi et al. 2019; Li et al. 1999).

Along the transects, SGD rates decrease with increasing water depths (Fig. 6C), which is caused by the interplay between the hydraulic gradient and seawater pressure. The increasing water pressure reduces the groundwater upward flow and limits the offshore extent of the seepage face. No data from the more seaward extension of the groundwater tube in the STEs is available. We expect convective seawater/groundwater mixing to be more important further offshore causing a higher S_{SGD} fraction.

Nutrient Distribution Along the Salinity Gradients and Fluxes

The varying strengths of nutrient sources and the microbial transformation of nutrients within the studied STE's are believed to be the main reasons for the variable nutrient concentrations along the salinity gradients of investigated STEs (Fig. 3). It is beyond the scope of this study to discuss these nutrient sources and biogeochemical transformation processes in detail. In general, we can state that apart from a land-derived, fresh groundwater (salinity < 1) nutrient source, a considerable part of nutrients is of autochthon marine origin. This is reflected in the DIN concentrations above the conservative mixing line between DIN in fresh groundwater and seawater (Fig. 7), and in comparably higher mean DIN (113 ± 207 µmol L^{-1}) and PO_4^{3-} (1.23 ± 0.23 µmol L^{-1}) concentrations in STE pore waters with salinities of 1–12 as compared to those in fresh groundwater (salinity < 1; DIN: 59.1 ± 68.3 µmol L^{-1}, PO_4^{3-}: 5.97 ± 11.9 µmol L^{-1}). The organic carbon content within sediments in the studied area was reported to be in the range between 0.5 and 2.5% (Balzer 1984) and mainly related to the presence of seagrass meadows (Boström et al. 2014) that are known to effectively store organic matter in sediments (Ricart et al. 2020). Ammonification and denitrification of organic matter, being the sequential reduction of NO_3^- to NH_4^+ (Voss et al. 2005; Korth et al. 2013) are the most likely processes causing the observed increase of ammonia in brackish groundwater of the STEs. Degradation of organic matter will also release PO_4^{3-} (Ahlgren et al. 2006) to the STE and PO_4^{3-} removal processes will spatially and temporally vary as depended on redox-conditions, which control PO_4^{3-} adsorption (Slomp and Van Cappellen 2004; van Helmond et al. 2020).

Other sources of organic matter may be organic-rich layers that formed during preglacial sedimentation and are now subject to leaching processes due to high freshwater and saltwater dynamics in the STE (Kreuzburg et al. 2018, 2020).

Our nutrient fluxes based on seepage meter measurements and radium mass balances agree within a factor of ~ 2 (DIN) and within a factor of ~ 5 for PO_4^{3-} (Table 3). Despite these relatively consistent fluxes, such estimates are associated with considerable uncertainties. For instance, collected waters in seepage meters may be subject to chemical modifications during the collection period, e.g., reduction of NO_3^- to NH_4^+ (Duque et al. 2020). Note that due to these possible chemical modifications we do not discuss N-species but only DIN fluxes. As recently pointed out by Garcia-Orellana et al. (2021), Ra-based SGD quantifications involve several, often unproven assumptions (e.g., steady-state, well-defined Ra source and sinks, diffusion-controlled Ra transport), that lead to unknown and not quantifiable uncertainties in SGD estimates. Most critical is the appropriate

choice of endmembers especially when calculating SGD-borne nutrient fluxes (Santos et al. 2008). In many studies, nutrient and Ra endmember concentrations are derived from fresh groundwater assuming that nutrients, like Ra, would behave conservatively while transported through the STE. Such an approach may be appropriate in systems characterized by rapid flushing through coarse-grained sediments and/or karstic environments (Santos et al. 2021). In most STE's, however, either nutrient attenuation via biogeochemical reactions or nutrient addition via circulating seawater and/or degradation of sedimentary organic matter occurs (Erler et al. 2014; Kroeger and Charette 2008; Oehler et al. 2021; Santos et al. 2009; Tait et al. 2014). In such cases, fresh groundwater nutrient endmembers are not an accurate expression of nutrient concentrations of discharging waters. As an alternative approach, we used the salinity range observed in seepage meters and assume that these ranges bracket the range of nutrient endmember concentrations. The calculated nutrient fluxes are about 2 (DIN) and ~ 10 times higher than the fluxes estimated from fresh groundwater endmembers (Table 4). These differences in the nutrient fluxes provide some guide on the potential amount of autochthonous nutrients. If fresh groundwater nutrients would pass though the STE biochemical reactor without modifications, about half of DIN and about one-tenth of PO_4^{3-} could be the maximal land-derived nutrient supply to Eckernförde Bay. Thus, the marine recycled nutrient source is likely to be more important. It should be noted that nutrients are also released from sediments via pore water diffusion (Carstensen et al. 2020). In Eckernförde Bay, diffusive pore-water DIN and PO_4^{3-} fluxes were estimated to be 1.4 ± 0.2 mmol m^{-2} d^{-1} and 0.7 ± 0.2 (Dale et al. 2011), respectively, which are lower (DIN) and in the same range (PO_4^{3-}) as our Ra based SGD estimates.

In the Bay of Puck (Baltic Sea), SGD-borne nutrient input of nitrogen and phosphorus (Szymczycha et al. 2012) was observed impacting meiofaunal communities (Kotwicki et al. 2014; Szymczycha et al. 2012). These authors reported SGD-derived DIN and PO_4^{3-} fluxes of 49.9 ± 18 t yr^{-1} and 1.72 ± 0.17 t yr^{-1}, respectively, which is in the range of our estimates (DIN: 38.4 ± 56.7 t yr^{-1}, PO_4^{3-}: 6.6 ± 12.0 t yr^{-1}).

The Baltic Sea is heavily impacted by external nutrient sources. Due to joint efforts of nations bordering the Baltic Sea, waterborne nitrogen and phosphorous inputs were reduced by 17% and 20%, respectively, between 1994 and 2010 (HELCOM 2015). In 2016, the riverine nitrogen and phosphorous input to the German Baltic Sea was estimated to be around 14,120 t y^{-1} and 500 t y^{-1}, respectively (HELCOM 2018). Scaling to the length of the German Baltic Sea coastline (2247 km), these inputs were 6.3 t km^{-1} y^{-1} of nitrogen and 0.2 t km^{-1} y^{-1} of phosphorous. If we assume

that our measured Ra- DIN and phosphorus fluxes are representative for the coastline (40 km) of Eckernförde Bay, the mean SGD-borne DIN fluxes are lower (mean DIN flux: 1 t km^{-1} y^{-1}, range: 0.1–4.7 t km^{-1} y^{-1}) and in the same range (PO_4^{3-} flux: 0.2 t km^{-1} y^{-1}, range: 0.1–0.9 t km^{-1} y^{-1}) as compared to the estimated total riverine inputs. This indicates that SGD derived DIN is not a major source exceeding the German riverine inputs. However, the freshwater supply by rivers in the Bay of Kiel is estimated at only 12%, whereas for other areas such as the Mecklenburg Bay, rivers such as the Warnow and Trave account for more than 50% of the freshwater supply (BLANO 2014). This makes statistically robust nutrient-runoff correlations for Kiel Bay Region less likely and may enhance the significance of SGD-derived nutrient inputs.

Our regional upscaling of fluxes to the entire Eckernförde Bay is associated with unknown uncertainties and probably still overestimates the "real" SGD-borne nutrient flux. For instance, cliffs consisting of tills with low permeability border part of the Eckernförde Bay coastline, and along such coastlines SGD is less likely. However, it should be noted that nutrient concentrations of the pore water of the STEs exceeded the defined target values (Kiel Bay: DIN < 22.2 µmol L^{-1} and P < 0.96 µmol L^{-1}) defined by HELCOM (2013c) for surface water of this region by a factor of 100 and may thus act as an additional source of nutrients due to the pronounced pore water dynamics. As already discussed above a considerable fraction of the SGD-borne nutrients might be of sedimentary or autochthon recycled marine origin. Therefore, the fraction of land-derived new nutrients contributing to the overall nutrient budget via SGD for the environmental status of the investigated area is difficult to distinguish and would require further studies for source determination.

Our nutrient fluxes determined for Eckernförde Bay fall in the range of a recent compilation of world-wide SGD rates (6.0 mmol m^{-2} d^{-1} for DIN and 0.1 mmol m^{-2} d^{-1} for PO_4^{-3}; Santos et al. 2021). These authors concluded that in up to 60% of their studied cases nutrient fluxes exceed river inputs. However, such an assessment is only meaningful if both sources (rivers and SGD) as well as the allochthonous land-derived nutrient fraction are considered. As shown in our study, a considerable part of SGD derived nutrients is of marine, recycled origin, indicating the presence of additional nutrient sources in our study area. As pointed out by Santos et al. (2021), most SGD studies failed to report these various nutrient fractions. In order to avoid overestimation of the SGD-derived and other individual nutrient inputs in the future, it is important to include and account for the additional nutrient sources on a regional basis to counteract the overall eutrophication of the Baltic Sea.

Conclusions

Our study identified a widespread occurrence of SGD along the coastline of Eckernförde Bay. We observed a STE structure different from most other previously studied STEs. Here we find a fresh groundwater tube which horizontally extends offshore and is overlaid by a seawater layer. Steep salinity gradients between fresh and saline waters are caused by the advection of fresh groundwater reducing density driven pore water circulation. This unique structure is most likely related to the microtidal environment and small waves in Eckernförde Bay causing a reduction of oceanic forces, which normally drive a considerable part of SGD in other ocean settings. In our study the main SGD driving force is the hydraulic gradient between land and sea, which is regulated by the wind-derived sea level changes. This setting favors elevated F_{SGD} fractions (up to 21%), which is remarkably high compared to other SGD studies. Thus, oceanic microtidal environments may be unique in the land–ocean water transport and resulting SGD.

Due to this high F_{SGD} fraction we would expect to see a much higher influence of allochthonous nutrients on the SGD composition. This is because F_{SGD} is mainly derived from the groundwater aquifers in the catchment area of Eckernförde Bay, which have high nutrient loadings. Instead, our study indicates that the land–ocean nitrogen transport does not exceed autochthon nutrient fluxes derived from organic matter recycling in sediments. The overall SGD-derived nitrogen inputs have only minor effect on the nutrient balance challenging the role of SGD as an important driver for eutrophication in the Baltic Sea. Thus, a high anthropogenic pressure in coastal zones may not necessarily imply a high impact of the solute transport associated with SGD. Future studies should more carefully investigate the various SGD nutrient sources (autochthonous versus allochthonous) in order to derive a more precise assessment on the role of SGD in oceanic nutrient budgets.

Data Availability Data is available on request.

References

Ahlgren, J., K. Reitzel, L. Tranvik, A. Gogoll, and E. Rydin. 2006. Degradation of organic phosphorus compounds in anoxic Baltic Sea sediments: A 31P nuclear magnetic resonance study. *Limnology and Oceanography* 51: 2341–2348.

Anderson Jr, W.P., and R.E. Emanuel. 2010. Effect of interannual climate oscillations on rates of submarine groundwater discharge. *Water Resources Research* 46.

Balzer, W. 1984. Organic matter degradation and biogenic element cycling in a nearshore sediment (Kiel Bight)1. *Limnology and Oceanography* 29: 1231–1246.

Beck, A.J., J.P. Rapaglia, J.K. Cochran, and H.J. Bokuniewicz. 2007. Radium mass-balance in Jamaica Bay, NY: evidence for a substantial flux of submarine groundwater. *Marine Chemistry* 106: 419–441. https://doi.org/10.1016/j.marchem.2013.03.002.

Black, F.J., A. Paytan, K.L. Knee, N.R. De Sieyes, P.M. Ganguli, E. Gray, et al. 2009. Submarine groundwater discharge of total mercury and monomethylmercury to central California coastal waters. *Environmental Science & Technology* 43:5652–5659. Available at: https://www.ncbi.nlm.nih.gov/pubmed/19731658.

BLANO. 2014. Harmonisierte Hintergrund- und Orientierungswerte für Nährstoffe und Chlorophyll-a in den deutschen Küstengewässern der Ostsee sowie Zielfrachten und Zielkonzentrationen für die Einträge über die Gewässer. Bonn: Bund/Länder-Ausschuss Nord- und Ostsee (BLANO).

Boström, C., S. Baden, A.-C. Bockelmann, K. Dromph, S. Fredriksen, C. Gustafsson, D. Krause-Jensen, T. Möller, S.L. Nielsen, B. Olesen, J. Olsen, L. Pihl, and E. Rinde. 2014. Distribution, structure and function of Nordic eelgrass (Zostera marina) ecosystems: Implications for coastal management and conservation. *Aquatic Conservation: Marine and Freshwater Ecosystems* 24: 410–434.

Breier J.A., H.N. Breier, H.N. Edmonds. 2005. Detecting submarine groundwater discharge with synoptic surveys of sediment resistivity, radium, and salinity. *Geophysical Research Letters* 32(23). https://doi.org/10.1029/2005GL024639.

Burnett, W.C., P.K. Aggarwal, A. Aureli, H. Bokuniewicz, J.E. Cable, M.A. Charette, et al. 2006. Quantifying submarine groundwater discharge in the coastal zone via multiple methods. *Science of the Total Environment* 367: 498–543. https://doi.org/10.1016/j.scitotenv.2006.05.009.

Burnett, W.C., M. Taniguchi, and J. Oberdorfer. 2001. Measurement and significance of the direct discharge of groundwater into the coastal zone. *Journal of Sea Research* 46: 109–116. https://doi.org/10.1016/S1385-1101(01)00075-2.

Bussmann, I., and E. Suess. 1998. Groundwater seepage in Eckernförde Bay (Western Baltic Sea): Effect on methane and salinity distribution of the water column. *Continental Shelf Research* 18: 1795–1806. https://doi.org/10.1016/S0278-4343(98)00058-2.

Carstensen, J., J.H. Andersen, B.G. Gustafsson, and D.J. Conley. 2014. Deoxygenation of the Baltic Sea during the last century. *Proceedings of the National Academy of Sciences USA* 111: 5628–5633. https://doi.org/10.1073/pnas.1323156111.

Carstensen, J., D.J. Conley, E. Almroth-Rosell, E. Asmala, E. Bonsdorff, V. Fleming-Lehtinen, B.G. Gustafsson, C. Gustafsson, A.-S. Heiskanen, U. Janas, A. Norkko, C. Slomp, A. Villnäs, M. Voss, and M. Zilius. 2020. Factors regulating the coastal nutrient filter in the Baltic Sea. *Ambio* 49: 1194–1210.

Charette, M.A., and M.C. Allen. 2006. Precision ground water sampling in coastal aquifers using a direct-push, shielded-screen well-point system. *Groundwater Monitoring & Remediation* 26:87–93. Available at: https://doi.org/10.1111/j.1745-6592.2006.00076.x.

Charette, M.A., E.R. Sholkovitz, and C.M. Hansel. 2005. Trace element cycling in a subterranean estuary: Part 1. Geochemistry of the permeable sediments. *Geochimica Et Cosmochimica Acta* 69: 2095–2109. https://doi.org/10.1016/j.gca.2004.10.024.

Cook, P.G., and D.K. Solomon. 1997. Recent advances in dating young groundwater: chlorofluorocarbons, 3H3He and 85Kr. *Journal of Hydrology* 191:245–265. Available at: http://citeseerx.ist.psu.edu/viewdoc/download?doi=10.1.1.455.3189&rep=rep1&type=pdf.

Couturier, M., G. Tommi-Morin, M. Sirois, A. Rao, C. Nozais, and G. Chaillou. 2017. Nitrogen transformations along a shallow subterranean estuary. *Biogeosciences* 14:3321. Available at: https://d-nb.info/1143063430/34.

Destouni, G., F. Hannerz, C. Prieto, J. Jarsjö, and Y. Shibuo. 2008. Small unmonitored near-coastal catchment areas yielding large mass loading to the sea. *Global Biogeochemical Cycles* 22. Available at: https://doi.org/10.1029/2008GB003287.

Dale, A.W., S. Sommer, L. Bohlen, T. Treude, V.J. Bertics, H.W. Bange, O. Pfannkuche, T. Schorp, M. Mattsdotter, and K. Wallmann. 2011. Rates and regulation of nitrogen cycling in seasonally hypoxic sediments during winter (Boknis Eck, SW Baltic Sea): Sensitivity to environmental variables. *Estuarine, Coastal and Shelf Science* 95: 14–28.

Duque, C., C.J. Russoniello, and D.O. Rosenberry. 2020. History and evolution of seepage meters for quantifying flow between groundwater and surface water: Part 2 – marine settings and submarine groundwater discharge. *Earth-Science Reviews* 204: 103168.

Erler, D.V., I.R. Santos, Y. Zhang, D.R. Tait, K.M. Befus, A. Hidden, L. Li, and B.D. Eyre. 2014. Nitrogen transformations within a tropical subterranean estuary. *Marine Chemistry* 164: 38–47.

Evans, T.B., and A.M. Wilson. 2016. Groundwater transport and the freshwater–saltwater interface below sandy beaches. *Journal of Hydrology* 538: 563–573.

Garcia-Orellana, J., V. Rodellas, J. Tamborski, M. Diego-Feliu, P. van Beek, Y. Weinstein, M. Charette, A. Alorda-Kleinglass, H.A. Michael, T. Stieglitz, and J. Scholten. 2021. Radium isotopes as submarine groundwater discharge (SGD) tracers: review and recommendations. *Earth-Science Reviews* 103681

Garcia-Solsona, E., P. Masqué, J. Garcia-Orellana, J. Rapaglia, A.J. Beck, J.K. Cochran, et al. 2008. Estimating submarine groundwater discharge around Isola La Cura, northern Venice Lagoon (Italy), by using the radium quartet. *Marine Chemistry* 109: 292–306. https://doi.org/10.1016/j.marchem.2008.02.007.

Ghyben, B.W. 1889. Nota in verband met de voorgenomen put boring nabij Amsterdam. Koninklijke Institute Ing Tijdschr p. 21.

Gonneea, M.E., A.E. Mulligan, and M.A. Charette. 2013. Seasonal cycles in radium and barium within a subterranean estuary: Implications for groundwater derived chemical fluxes to surface waters. *Geochimica et Cosmochimica Acta* 119: 164–177. https://doi.org/10.1016/j.gca.2013.05.034

Greskowiak, J. 2014. Tide-induced salt-fingering flow during submarine groundwater discharge. *Geophysical Research Letters* 41: 6413–6419. Available at: https://doi.org/10.1002/2014GL061184.

Hannerz, F., and G. Destouni. 2006. Spatial characterization of the Baltic sea drainage basin and its unmonitored catchments. *Ambio* 35: 214–219. Available at: https://www.ncbi.nlm.nih.gov/pubmed/16989505.

HELCOM. 2013c. Review of the Fifth Baltic Sea Pollution Load Compilation for the 2013 HELCOM Ministerial Meeting. Baltic Sea Environment Proceedings No. 141.HELCOM 2012. Fifth Baltic Sea Pollution Load Compilation – An Executive Summary. Baltic Sea Environment Proceedings No. 128A.

HELCOM. 2015. Updated Fifth Baltic Sea pollution load compilation (PLC-5.5). No. 145. *Baltic Sea Environment Proceedings* No. 145.

HELCOM. 2018. Sources and pathways of nutrients to the Baltic Sea. *Baltic Sea Environment Proceedings* No. 153.

Hoffmann, J.J.L., J. Schneider von Deimling, J.F. Schröder, M. Schmidt, P. Held, G.J. Crutchley, et al. 2020. Complex eyed pockmarks and submarine groundwater discharge revealed by acoustic data and sediment cores in Eckernförde Bay, SW Baltic Sea. *Geochemistry, Geophysics, Geosystems* 21: 16. https://doi.org/10.1029/2019GC008825.

Hu, C., F.E. Muller-Karger, and P.W. Swarzenski. 2006. Hurricanes, submarine groundwater discharge, and Florida's red tides. *Geophysical Research Letters* 33: 591. https://doi.org/10.1029/2005GL025449.

Idczak, J., A. Brodecka-Goluch, K. Łukawska-Matuszewska, B. Graca, N. Gorska, Z. Klusek, P.D. Pezacki, and J. Bolałek. 2020. A geophysical, geochemical and microbiological study of a newly discovered pockmark with active gas seepage and submarine groundwater discharge (MET1-BH, central Gulf of Gdańsk, southern Baltic Sea). *Science of the Total Environment* 742: 140306.

Jensen, J.B., A. Kuijpers, O. Bennike, T. Laier, and F. Werner. 2002. New geological aspects for freshwater seepage and formation in Eckernförde Bay, western Baltic. *Continental Shelf Research* 22: 2159–2173. https://doi.org/10.1016/S0278-4343(02)00076-6.

Johannes, R.E. 1980. The ecological significance of the submarine discharge of groundwater. *Marine Ecology Progress Series* 3: 365–373. Available at: http://www.jstor.org/stable/24813143.

Kaleris, V., G. Lagas, S. Marczinek, J. Piotrowski, and a. 2002. Modelling submarine groundwater discharge: An example from the western Baltic Sea. *Journal of Hydrology* 265: 76–99. https://doi.org/10.1016/S0022-1694(02)00093-8.

Kérouel, R., and A. Aminot. 1997. Fluorometric determination of ammonia in sea and estuarine waters by direct segmented flow analysis. *Marine Chemistry* 57: 265–275. https://doi.org/10.1016/S0304-4203(97)00040-6.

Kłostowska, Ż, B. Szymczycha, M. Lengier, D. Zarzeczańska, and L. Dzierzbicka-Głowacka. 2020. Hydrogeochemistry and magnitude of SGD in the Bay of Puck, southern Baltic Sea. *Oceanologia* 62: 1–11. https://doi.org/10.1016/j.oceano.2019.09.001.

Korth, F., B. Fry, I. Liskow, and M. Voss. 2013.Nitrogen turnover during the spring outflows of the nitrate-rich Curonian and Szczecin lagoons using dual nitrate isotopes. *Marine Chemistry* 154: 1–11.https://doi.org/10.1016/j.marchem.2013.04.012

Kotwicki, L., K. Grzelak, M. Czub, O. Dellwig, T. Gentz, B. Szymczycha, et al. 2014. Submarine groundwater discharge to the Baltic coastal zone: Impacts on the meiofaunal community. *Journal of Marine Systems* 129: 118–126. https://doi.org/10.1016/j.jmarsys.2013.06.009.

Krall, L., G. Trezzi, J. Garcia-Orellana, V. Rodellas, C.-M. and Mörth, P. 2017. Andersson Submarine groundwater discharge

at Forsmark, Gulf of Bothnia, provided by Ra isotopes. *Marine Chemistry* 196: 162–172. https://doi.org/10.1016/j.marchem.2017.09.003.

Kreuzburg, M., M. Ibenthal, M. Janssen, G. Rehder, M. Voss, M. Naumann, et al. 2018. Sub-marine continuation of peat deposits from a Coastal Peatland in the Southern Baltic Sea and its Holocene Development. *Frontiers in Earth Science* 6: 103. https://doi.org/10.3389/feart.2018.00103.

Kreuzburg, M., F. Rezanezhad, T. Milojevic, M. Voss, L. Gosch, S. Liebner, et al. 2020. Carbon release and transformation from coastal peat deposits controlled by submarine groundwater discharge: A column experiment study. *Limnology and Oceanography* 65 (5): 1116–1135. https://doi.org/10.1002/lno.11438.

Kroeger, K.D., M. Charette, and a. 2008. Nitrogen biogeochemistry of submarine groundwater discharge. *Limnology and Oceanography* 53: 1025–1039. https://doi.org/10.4319/lo.2008.53.3.1025.

LaRoche, J., R. Nuzzi, R. Waters, and K. Wyman. 1997. Brown tide blooms in Long Island's coastal waters linked to interannual variability in groundwater flow. Glob. Chang. Biol. Available at: https://doi.org/10.1046/j.1365-2486.1997.00117.x.

Lee, D.R. 1977. A device for measuring seepage flux in lakes and estuaries. *Limnology and Oceanography* 22: 140–147. https://doi.org/10.4319/lo.1977.22.1.0140.

Lee, Y.-W., G. Kim, W.-A. Lim, and D.-W. Hwang. 2010. A relationship between submarine groundwater borne nutrients traced by Ra isotopes and the intensity of dinoflagellate red-tides occurring in the southern sea of Korea. *Limnology and Oceanography* 55: 1–10. https://doi.org/10.4319/lo.2010.55.1.0001.

Li, L., D.A. Barry, F. Stagnitti, and J.-Y. Parlange. 1999. Submarine groundwater discharge and associated chemical input to a coastal sea. *Water Resources Research* 35: 3253–3259. https://doi.org/10.1029/1999WR900189

LLUR – Landesamt für Landwirtschaft, Umwelt und ländliche Räume, Schleswig-Holstein. 2020. Landschafts- und Umweltatlas: Umwelt http://www.umweltdaten.landsh.de/atlas/script/index.php. (Accessed on 1 April 2021)

Luijendijk, E., T. Gleeson, and N. Moosdorf. 2020. Fresh groundwater discharge insignificant for the world's oceans but important for coastal ecosystems. *Nature Communications* 11: 1260. https://doi.org/10.1038/s41467-020-15064-8.

Marczinek, S. and J.A. Piotrowski. 2002. Grundwasserströmung und -beschaffenheit im Einzugsgebiet der Eckernförder Bucht, Schleswig-Holstein. *Grundwasser* 101–110.

McAllister, S.M., J.M. Barnett, J.W. Heiss, A.J. Findlay, D.J. MacDonald, C.L. Dow, et al. 2015. Dynamic hydrologic and biogeochemical processes drive microbially enhanced iron and sulfur cycling within the intertidal mixing zone of a beach aquifer. *Limnology and Oceanography* 60: 329–345. Available at: https://doi.org/10.1002/lno.10029.

Moore, W.S. 1999. The subterranean estuary: A reaction zone of ground water and sea water. *Marine Chemistry* 65: 111–125. https://doi.org/10.1016/S0304-4203(99)00014-6.

Moore, W.S. 2000. Determining coastal mixing rates using radium isotopes. *Continental Shelf Research* 20: 1993–2007. https://doi.org/10.1016/S0278-4343(00)00054-6.

Moore, W.S. 2003. Sources and fluxes of submarine groundwater discharge delineated by radium isotopes. *Biogeochemistry* 66: 75–93. https://doi.org/10.1023/B:BIOG.0000006065.77764.a0.

Moore, W.S. 2006. Radium isotopes as tracers of submarine groundwater discharge in Sicily. *Continental Shelf Research* 26: 852–861. https://doi.org/10.1016/j.csr.2005.12.004.

Moore, W.S. 2010. The effect of submarine groundwater discharge on the ocean. *Annual Review of Marine Science* 2: 59–88. https://doi.org/10.1146/annurev-marine-120308-081019.

Moore, W.S., J.L. Sarmiento, and R.M. Key. 2008. Submarine groundwater discharge revealed by 228Ra distribution in the upper Atlantic Ocean. *Nature Geoscience* 1: 309–311. https://doi.org/10.1038/ngeo183.

Moore, W.S., and P. Cai. 2013. Calibration of RaDeCC systems for 223Ra measurements. *Marine Chemistry* 156: 130–137. https://doi.org/10.1016/j.marchem.2013.03.002

Moore, W.S., and R. Arnold. 1996. Measurement of 223Ra and 224Ra in coastal waters using a delayed coincidence counter. *Journal Geophysical Research* 101: 1321–1329. https://doi.org/10.1029/95JC03139

Moore, W.S. and S.B. Joye. 2021. Saltwater intrusion and submarine groundwater discharge: acceleration of biogeochemical reactions in changing coastal aquifers. *Frontiers in Earth Science* 9.

Oehler, T., M. Ramasamy, M.E. George, S.D.S. Babu, K. Dähnke, M. Ankele, M.E. Böttcher, I.R. Santos, and N. Moosdorf. 2021. Tropical beaches attenuate groundwater nitrogen pollution flowing to the ocean. *Environmental Science & Technology*.

Pempkowiak, J., B. Szymczycha, and L. Kotwicki. 2010. Submarine groundwater discharge (SGD) to the Baltic Sea. *Rocznik Ochrona Środowiska* 12: 17–32. Available at: http://www.wbiis.tu.koszalin.pl/towarzystwo/text/pp_2010_001.pdf.

Peng, T., J. Liu, X. Yu, F. Zhang, and J. Du. 2022. Assessment of submarine groundwater discharge (SGD) and associated nutrient subsidies to Xiangshan Bay (China), an aquaculture area, Journal of Hydrology, Volume 610. *ISSN* 127795: 0022–1694. https://doi.org/10.1016/j.jhydrol.2022.127795.

Piekarek-Jankowska, H. 1996. Hydrochemical effects of submarine groundwater discharge to the Puck Bay [Southern Baltic Sea, Poland]. *Geographia Polonica* 67. Available at: http://agro.icm.edu.pl/agro/element/bwmeta1.element.agro-article-47dd0e15-8453-40c4-a503-d9afa03b0fc0.

Rahman, M.M., Y.-G. Lee, G. Kim, K. Lee, and S. Han. 2013. Significance of submarine groundwater discharge in the coastal fluxes of mercury in Hampyeong Bay, Yellow Sea. *Chemosphere* 91: 320–327. https://doi.org/10.1016/j.chemosphere.2012.11.052.

Rapaglia, J.P., and H.J. Bokuniewicz. 2009. The effect of groundwater advection on salinity in pore waters of permeable sediments. *Limnology and Oceanography* 54: 640–643. https://doi.org/10.4319/lo.2009.54.2.0630.

Renger, M., and G. Wessolek. 1990. Auswirkungen von Grundwasserabsenkung auf die Grundwasserneubildung.- Mitteilungen des Instituts für Wasserwesen, Bd. 386: S. 295 - 307, München.

Ricart, A.M., P.H. York, C.V. Bryant, M.A. Rasheed, D. Ierodiaconou, and P.I. Macreadie. 2020. High variability of Blue Carbon storage in seagrass meadows at the estuary scale. *Scientific Reports* 10: 5865.

Robinson, C.E., P. Xin, I.R. Santos, M.A. Charette, L. Li, and D.A. Barry. 2018. Groundwater dynamics in subterranean estuaries of coastal unconfined aquifers: Controls on submarine groundwater discharge and chemical inputs to the ocean. *Advances in Water Resources* 115: 315–331. https://doi.org/10.1016/j.advwatres.2017.10.041.

Robinson, C., L. Li, and D.A. Barry. 2007a. Effect of tidal forcing on a subterranean estuary. *Advances in Water Resources*. 30: 851–865. https://doi.org/10.1016/j.advwatres.2006.07.006.

Robinson, C., L. Li, and H. Prommer. 2007b. Tide-induced recirculation across the aquifer-ocean interface. *Water Resources Research* 43: n/a-n/a.

Rocha, C., J. Wilson, J. Scholten, and M. Schubert. 2015. Retention and fate of groundwater-borne nitrogen in a coastal bay (Kinvara Bay, Western Ireland) during summer. *Biogeochemistry* 125: 275–299. https://doi.org/10.1007/s10533-015-0116-1.

Rodellas, V., J. Garcia-Orellana, P. Masqué, M. Feldman, and Y. Weinstein. 2015. Submarine groundwater discharge as a major source of nutrients to the Mediterranean Sea. *Proceedings of the National Academy of Sciences* 112: 3926–3930.

Röper, T., J. Greskowiak, and G. Massmann. 2015. Instabilities of submarine groundwater discharge under tidal forcing. *Limnology and Oceanography* 60: 22–28. https://doi.org/10.1002/lno.10005.

Russoniello, C.J., and H.A. Michael. 2015. Investigation of seepage meter measurements in steady flow and wave conditions. *Ground Water* 53: 959–966. https://doi.org/10.1111/gwat.12302.

Santos, I.R., W.C. Burnett, J. Chanton, B. Mwashote, I.G.N. Suryaputra, and a., and Dittmar, T. 2008. Nutrient biogeochemistry in a Gulf of Mexico subterranean estuary and groundwater-derived fluxes to the coastal ocean. *Limnology and Oceanography* 53: 705–718. https://doi.org/10.4319/lo.2008.53.2.0705.

Santos, I.R., W.C. Burnett, T. Dittmar, I.G.N.A. Suryaputra, and J. Chanton. 2009. Tidal pumping drives nutrient and dissolved organic matter dynamics in a Gulf of Mexico subterranean estuary. *Geochimica Et Cosmochimica Acta* 73: 1325–1339. https://doi.org/10.1016/j.gca.2008.11.029.

Santos, I.R., B.D. Eyre, and M. Huettel. 2012. The driving forces of porewater and groundwater flow in permeable coastal sediments: A review. *Estuarine, Coastal and Shelf Science* 98: 1–15. https://doi.org/10.1016/j.ecss.2011.10.024.

Santos, I.R., X. Chen, A.L. Lecher, A.H. Sawyer, N. Moosdorf, V. Rodellas, J. Tamborski, H.-M. Cho, N. Dimova, R. Sugimoto, S. Bonaglia, H. Li, M.-C. Hajati, and L. Li. 2021. Submarine groundwater discharge impacts on coastal nutrient biogeochemistry. *Nature Reviews Earth & Environment*.

Schafmeister, M.-T., and Darsow, A. (2011). "Potential change in groundwater discharge as response to varying climatic conditions--an experimental model study at catchment scale," in The Baltic Sea Basin (Springer), 391–404. Available at: https://link.springer.com. https://doi.org/10.1007/978-3-642-17220-5_19.

Schlosser, P., Shapiro, S. D., Stute, M., Aeschbach-Hertig, W., Plummer, N., and Busenberg, E. (1998). Tritium/3He measurements in young groundwater. Chronologies for environmental records. in Isotope techniques in the study of environmental change. Proceedings of a symposium, Vienna, April 1997. (International Atomic Energy Agency), 165–189. Available at: https://asu.pure.elsevier.com/en/publications/tritiumsup3suphe-measurements-in-young-groundwater-chronologies-f.

Schlüter, M., E.J. Sauter, C.E. Andersen, H. Dahlgaard, and P.R. Dando. 2004. Spatial distribution and budget for submarine groundwater discharge in Eckernförde Bay (Western Baltic Sea). *Limnology and Oceanography* 49: 157–167. https://doi.org/10.4319/lo.2004.49.1.0157.

Scholten, J.C., M.K. Pham, O. Blinova, M.A. Charette, H. Dulaiova, and M. Eriksson. 2010. Preparation of Mn-fiber standards for the efficiency calibration of the delayed coincidence counting system (RaDeCC). *Marine Chemistry* 121: 206–214. https://doi.org/10.1016/j.marchem.2010.04.009.

Seeberg-Elverfeldt, J., Schlüter, M., Feseker, T., and Kölling, M. (2005). Rhizon sampling of porewaters near the sediment-water interface of aquatic systems. Limnol. Oceanogr. Methods 3, 361–371. Available at: http://onlinelibrary.wiley.com. https://doi.org/10.4319/lom.2005.3.361/full.

Seibold, E., Exon, N., Hartmann, M., Kögler, F.-C., Krumm, H., Lutze, G. F., et al. (1971). "Marine geology of Kiel bay," in (Kramer). Available at: http://oceanrep.geomar.de/27367/1/1971_Seibold_MarGeol-Kiel-Bay_SedimentologyCentralEurope.pdf.

Seitzinger, S.P., J.A. Harrison, and E. Dumont. 2005. Sources and delivery of carbon, nitrogen, and phosphorus to the coastal zone: an overview of Global Nutrient Export from Watersheds (NEWS) models and their …. Global. Available at: https://doi.org/10.1029/2005gb002606.

Shaw, R.D., and E.E. Prepas. 1989. Anomalous, short-term influx of water into seepage meters. *Limnology and Oceanography* 34: 1343–1351. Available at: https://doi.org/10.4319/lo.1989.34.7.1343.

Slomp, C.P., and P. Van Cappellen. 2004. Nutrient inputs to the coastal ocean through submarine groundwater discharge: Controls and potential impact. *Journal of Hydrology* 295: 64–86. https://doi.org/10.1016/j.jhydrol.2004.02.018.

Sültenfuβ, J., R. Purtschert, and J.F. Führböter. 2011. Age structure and recharge conditions of a coastal aquifer (northern Germany) investigated with ^{39}Ar, ^{14}C, ^{3}H, He isotopes and Ne. *Hydrogeology Journal* 19: 221–236. https://doi.org/10.1007/s10040-010-0663-4.

Sültenfuß, J., W. Roether, and M. Rhein. 2009. The Bremen mass spectrometric facility for the measurement of helium isotopes, neon, and tritium in water. *Isotopes in Environmental and Health Studies* 45: 83–95. https://doi.org/10.1080/10256010902871929.

Szymczycha, B., S. Vogler, and J. Pempkowiak. 2012. Nutrient fluxes via submarine groundwater discharge to the Bay of Puck, southern Baltic Sea. *Science of the Total Environment* 438: 86–93. https://doi.org/10.1016/j.scitotenv.2012.08.058.

Taniguchi, M. 2002. Tidal effects on submarine groundwater discharge into the ocean. *Geophysical Research Letters* 29: 9–11. https://doi.org/10.1029/2002GL014987.

Taniguchi, M., H. Dulai, K.M. Burnett, I.R. Santos, R. Sugimoto, T. Stieglitz, et al. 2019. Submarine groundwater discharge: Updates on its measurement techniques, geophysical drivers, magnitudes, and effects. *Frontiers of Environmental Science & Engineering in China* 7: 141. https://doi.org/10.3389/fenvs.2019.00141.

Tait, D.R., D.V. Erler, I.R. Santos, T.J. Cyronak, U. Morgenstern, and B.D. Eyre. 2014. The influence of groundwater inputs and age on nutrient dynamics in a coral reef lagoon. *Marine Chemistry* 166: 36–47.

Tolstikhin, I.N., and I.L. Kamensky. 1969. On the possibility of tritium-helium-3 dating of underground waters. *Geokhimiya* 8 (1027): 1029.

Vanek, V., and D.R. Lee. 1991. Mapping submarine groundwater discharge areas: an example from Laholm Bay, southwest Sweden. *Limnology and Oceanography* 36: 1250–1262. Available at: https://pascal-francis.inist.fr/vibad/index.php?action=getRecordDetail&idt=5413124.

van Helmond, N.A.G.M., E.K. Robertson, D.J. Conley, M. Hermans, C. Humborg, L.J. Kubeneck, W.K. Lenstra, and C.P. Slomp. 2020. Removal of phosphorus and nitrogen in sediments of the eutrophic Stockholm archipelago, Baltic Sea. *Biogeosciences* 17: 2745–2766.

Vaupotic, J., A. Gregoric, J. Kotnik, M. Horvat, and N. Pirrone. 2008. Dissolved radon and gaseous mercury in the Mediterranean seawater. *Journal of Environmental Radioactivity* 99: 1068–1074. https://doi.org/10.1016/j.jenvrad.2007.12.023.

Virtasalo, J., J. Schröder, S. Luoma, N. Hendriksson, and J. Scholten. 2019. Stable isotope study of submarine groundwater discharge at the Hanko Peninsula, south Finland. in Geophysical.

von Ahn, C.M.E., J.C. Scholten, C. Malik, P. Feldens, B. Liu, O. Dellwig, A.-K. Jenner, S. Papenmeier, I. Schmiedinger, M.A. Zeller, and M.E. Böttcher. 2021. A multi-tracer study of fresh water sources for a temperate urbanized coastal bay (Southern Baltic Sea). *Frontiers in Environmental Science* 9.

Voss, M., K.-C. Emeis, S. Hille, T. Neumann, and J.W. Dippner. 2005. Nitrogen cycle of the Baltic Sea from an isotopic perspective. *Global Biogeochemical Cycles* 19. https://doi.org/10.1029/2004GB002338

Wasmund, N., and H. Siegel. 2008. Phytoplankton. In *State and evolution of the Baltic Sea, 1952–2005*, ed. R. Feistel, G. Nausch, and N. Wasmund, 441–481. Hoboken, New Jersey: John Wiley and Sons.

Whiticar, M.J., and F. Werner. 1981. Pockmarks: Submarine vents of natural gas or freshwater seeps? *Geo-Marine Letters* 1: 193–199. https://doi.org/10.1007/BF02462433.